

BCS CLASS II DRUG DISPERSIONS IN  
HYDROXYPROPYL METHYLCELLULOSE SOLUTIONS:  
THE EFFECT OF POLYMER MOLECULAR WEIGHT AND  
DRUG LOADING ON THE STEADY-STATE RHEOLOGY  
OF HPMC SOLUTIONS

By

Mariel M. Santiago-Vázquez

A thesis submitted in partial fulfillment of the requirements for the degree of

MASTER OF SCIENCE

in

Chemical Engineering

University of Puerto Rico

Mayagüez Campus

2015

\_\_\_\_\_  
Dr. Aldo Acevedo, Ph.D.  
President Graduate Committee

\_\_\_\_\_  
Date

\_\_\_\_\_  
Dr. Rafael Méndez, Ph.D.  
Member, Graduate Committee

\_\_\_\_\_  
Date

\_\_\_\_\_  
Dr. Jorge L. Almodóvar, Ph.D.  
Member, Graduate Committee

\_\_\_\_\_  
Date

\_\_\_\_\_  
Profa. Sandra Zapata  
Graduate School Representative

\_\_\_\_\_  
Date

\_\_\_\_\_  
Dr. Aldo Acevedo, Ph.D.  
Chairperson of the Department

\_\_\_\_\_  
Date

## ABSTRACT

Physical biopolymer gels are ideal candidates for the drug delivery of solid pharmaceutical drugs. Nevertheless, inclusion of particles may affect the rheology and gelation of these systems. In this work, we evaluate the effects of particle loading on the steady-state viscosity of a model biopolymer-particle system. The studied system consists of hydroxypropyl methylcellulose (HPMC) of two different grades, E4M and E15LV, and two BCS Class II drugs, griseofulvin and naproxen. The effect of particle size was studied using various particle size ranges of naproxen ( $d < 45 \mu\text{m}$ ,  $45\text{-}75 \mu\text{m}$ ,  $75\text{-}125 \mu\text{m}$ , and  $> 125 \mu\text{m}$ ). For HPMC E15LV a Newtonian behavior was observed, while HPMC E4M behaved as a Bingham pseudoplastic. Overall, the effect of particle inclusion into the biopolymer led to a decrease in both viscosity and yield stress for both HPMC viscosity grades. The decrease in viscosity was attributed to the adsorption of polymer to the particle surface and the decrease in yield stress was attributed to a decrease in polymer-polymer interaction.

## RESUMEN

Los geles físicos de biopolímeros son candidatos ideales para la administración de fármacos sólidos. Sin embargo, la inclusión de partículas podría afectar la reología y gelación de estos sistemas. En este trabajo, estudiamos el efecto de la inclusión de partículas en la viscosidad en estado estacionario de un sistema modelo de biopolímero-droga. El sistema estudiado consistió de dos distintos grados de hidroxipropil metilcelulosa (HPMC), E15LV y E4M, y dos drogas BCS tipo II, griseofulvin y naproxen. Para ver el efecto del tamaño de partícula en la viscosidad del polímero, se utilizaron varios rangos de tamaño de naproxen ( $d < 45 \mu\text{m}$ ,  $45\text{-}75 \mu\text{m}$ ,  $75\text{-}125 \mu\text{m}$ , and  $> 125 \mu\text{m}$ ). Para HPMC E15LV se observó comportamiento Newtoniano, mientras que HPMC E4M mostró un comportamiento pseudoplástico de Bingham. En general, la adición de particulado al sistema de HPMC causó una disminución en la viscosidad y el esfuerzo de rendición para las concentraciones estudiadas de HPMC. Esta disminución en viscosidad se debe a la adsorción del polímero en la superficie de la partícula y la disminución del esfuerzo de rendición se debe a una disminución de interacción polímero-polímero.

To my Dad

Who always believed in me and gave me the push needed to continue

Even though you are unable to see the end result of my work,

This is for you

## ACKNOWLEDGMENTS

I would like to thank my advisor, Dr. Aldo Acevedo, for motivating me as an undergraduate student to continue into graduate studies. I really appreciate all your mentoring, guidance, advice and support through out this process.

I want to thank my lab-mates for their support, suggestions and collaborations throughout this project. Thanks particularly to Ana Cameron, without whom this experience would have been completely different. Ana, thank you for your willingness to help, for being a sounding board when I needed to bounce off ideas, for your guidance, mentorship, and, most importantly, for your friendship.

I want to thank the Department of Chemical Engineering and the NSF-sponsored ERC SOPS for the financial support, professional exposure and educational opportunities offered throughout these past years.

To my family and friends, thank you for their support and understanding throughout this process. To my parents and my sister, thank you for always supporting and motivating me and for being my strength in times of need. Frank and Lizzette, who could understand me better than you two? Thank you for your support and for always being available to share the hardships, triumphs and joys of this experience.

To my loving husband, Ernesto, thank you for supporting me and being my rock when times proved to be more challenging. Thank you for always believing in me and for being my biggest supporter. I love you dearly.

Last, but not least, I want to thank my professors and committee members for their suggestions and support throughout this endeavor.

## TABLE OF CONTENTS

ABSTRACT .....	ii
RESUMEN .....	iii
LIST OF TABLES .....	viii
LIST OF FIGURES .....	ix
1 Introduction .....	1
2 Background.....	4
2.1 Cellulose and its Derivatives .....	5
2.2 Hydroxypropyl methylcellulose .....	10
2.3 BCS Class II Drugs .....	39
2.4 Negative Deviation from the Einstein Viscosity Model .....	42
3 Materials and Experimental Method .....	45
3.1 Hydroxypropyl methylcellulose .....	45
3.2 BCS Class II Model Drugs: Griseofulvin and Naproxen .....	46
3.2.1 Drug Characterization .....	47
3.2.1.1 Particle Size Determination .....	47
3.2.1.2 Thermal Transitions.....	49
3.3 HPMC Sample Preparation .....	49
3.3.1 Densitometry .....	50
3.4 Rheological Measurements .....	51
4 Results and Discussion .....	52
4.1 Steady-state viscosity of HPMC solutions loaded with griseofulvin .....	52
4.2 Steady-state viscosity of HPMC solutions loaded with naproxen .....	60
5 Conclusion.....	66
REFERENCES .....	68

A	APPENDIX .....	74
---	----------------	----

## LIST OF TABLES

Table 2.1: Substituents of water-soluble cellulose esters .....	8
Table 2.2: Substituents of water-soluble cellulose ethers.....	8
Table 2.3: Substituents of water-soluble mixed ethers.....	8
Table 2.4: Physicochemical properties of the drugs.....	10
Table 2.5: USP specification for different type of HPMC, classified according to their degree of methoxy and hydroxypropyl substitution.....	12
Table 2.6: Various grades of HPMC.....	12
Table 2.7: Composition for Methocel cellulose derivatives used by Haque and Morris.....	13
Table 2.8: HPMC batches and their properties.....	33
Table 2.9: Values of Cross parameters at different concentrations for HPMC solutions at 25°C.....	34
Table 2.10: Polymer characteristics of the four HPMC batches.....	37
Table 2.11: The Biopharmaceutics Classification System.....	39
Table 2.12: Classification of orally administered drugs on the WHO model list of Essential Medicines according to the BCS: <i>Drugs with reliable solution and permeability data</i> .....	41
Table 3.1: Physical properties of HPMCs as provided by distributor .....	45
Table 3.2: Particle size distribution for naproxen .....	48
Table 3.3: Solution densities for Griseofulvin, unsieved Naproxen and sieved Naproxen in HPMC E4M and E15LV solutions.....	51



## LIST OF FIGURES

Figure 2.1: Structure of native cellulose.....	6
Figure 2.2: Structure of water-soluble cellulose derivatives (R=H or R from table 2.1 or 2.2) .....	7
Figure 2.3: Cellulose derivative structures: (a) CMC and (b) HPC .....	7
Figure 2.4: Chemical structure of hydroxypropyl methylcellulose.....	9
Figure 2.5: Chemical Structure of drug molecules: (a) griseofulvin and (b) naproxen.....	9
Figure 2.6: DSC traces for 2% (w/v) methylcellulose and HPMC from Haque and Morris on (a) heating and (b) cooling at 0.1 deg min <sup>-1</sup> .....	15
Figure 2.7: Shear thinning behavior of 2% (w/v) E4M plotted as $\eta$ vs. $\eta\gamma^p$ for (a) $p=0.76$ and (b) $p=0.56$ .....	16
Figure 2.8: Generalized shear thinning behavior of Methocel samples A4M (n), E4M ( $\Delta$ ), F4M ( $\square$ ) and K4M (*); (a) steady-shear viscosity; (b) complex dynamic viscosity; $\eta=\eta_0/2$ at $\gamma=\gamma_{1/2}$ ; $\eta^*=\eta^*_0/2$ at $\omega=\omega_{1/2}$ .....	17
Figure 2.9: Thermorheogram of a 2% (w/v) (a) and 20% w/v (b) HPMC E4M system.....	19
Figure 2.10: Frequency sweeps of 2% E4M solutions at 25 (a), 55 (b) and 85°C (c)..	20
Figure 2.11: Storage ( $G'$ , squares), loss ( $G''$ , circles) and the complex viscosity ( $\eta^*$ , triangles) modulus, as a function of temperature, for HPMC solutions of (a) 1%, (b) 2%, (c) 5% and (d) 10% w/w. Frequency is chosen so as to impose a value of $G''$ higher than $G'$ at the initial conditions.....	22
Figure 2.12: The influence of temperature on the $G'$ and $G''$ values for a 4% solution of a 4000mPa viscosity grade HPMC polymer with DS of 1.85 and MS of 0.16 at a frequency of 1 Hz and 8.5 % amplitude heated at a scan rate of 1C min <sup>-1</sup> .....	23

Figure 2.13: Evolution of elastic ( $G'$ ) and viscous ( $G''$ ) moduli upon heating and cooling HPMC solution (pH 7). $T_{gel}$ : gelation temperature; $T_m$ : melting temperature. ....	24
Figure 2.14: The effect of temperature on the viscoelastic moduli and $\tan \delta$ of 2% w/w HPMC solutions during (a) heating and (b) cooling cycles. ....	26
Figure 2.15: Gelation temperature of 1 wt% aqueous HPMC solutions as a function of SDS concentration in the absence (n) or presence (■) of 1 wt% griseofulvin. ....	28
Figure 2.16: Zero-shear steady state viscosity of aqueous HPMC solutions at 1 wt% with SDS in the absence (n) or presence (■) of 1 wt% griseofulvin.....	29
Figure 2.17: Schematic representations showing the interactions between HPMC, SDS, and griseofulvin at $T_1$ and $T_2$ , where $T_1 < T_{gel} < T_2$ . Panes (a) and (b) represent the system with no SDS; panes (c) and (d) represent the system with limited concentration of SDS; and panels (e) and (f) represent the system with higher concentration of SDS, but below the critical micelle concentration. ....	30
Figure 2.18: Viscosity dependence on temperature for HPMC solutions of (a) 1%, (b) 2%, (c) 5% and (d) 10%, w/w. Curves are obtained at Newtonian shear rates (triangles), with imposed values respectively of 0.5, 0.05, $5.0 \times 10^{-3}$ and $1.0 \times 10^{-3} \text{ s}^{-1}$ , and non-Newtonian shear rates (circles, of 50, 30, 5 and $1 \text{ s}^{-1}$ respectively. ....	32
Figure 2.19: The continuous shear viscosity of 1% HPMC solutions with respect to drug concentration (A) meclufenamate Na and (B) diclofenac Na. Measurements at $20 \pm 0.1^\circ\text{C}$ .. ....	36
Figure 2.20: Flow curves obtained at $37^\circ\text{C}$ . (A) 5% (w/w) HPMC solutions and (B) 10% (w/w) HPMC solutions. (■) Batch A, (□) Batch B, (filled $\Delta$ ) Batch C and ( $\Delta$ ) Batch D. ....	38
Figure 3.1: Zeta Potential for aqueous HPMC solutions with griseofulvin and naproxen .....	47
Figure 3.2: Particle size distribution for naproxen particles.....	48

Figure 4.1: Steady-state viscosity of aqueous 2 wt% HPMC E15LV solution as a function of shear rate and griseofulvin concentration at 25°C .....	53
Figure 4.2: Newtonian viscosity for aqueous 2 wt% HPMC E15LV solution as a function of griseofulvin concentration at 25°C .....	53
Figure 4.3: Steady-state viscosity of aqueous 2 wt% HPMC E4M solution as a function of shear rate and griseofulvin concentration at 25°C .....	55
Figure 4.4: Plateau viscosity, $\mu_0$ , from fitted Bingham model to steady-state viscosity of aqueous 2 wt% HPMC E4M solution as a function of shear rate and griseofulvin concentration at 25°C .....	56
Figure 4.5: Yield stress, $\tau_y$ , from fitted Bingham model to steady-state viscosity of aqueous 2 wt% HPMC E4M solution as a function of shear rate and griseofulvin concentration at 25°C .....	57
Figure 4.6: Steady-state viscosity of aqueous 1 wt% HPMC E4M solution as a function of shear rate and griseofulvin concentration at 25°C .....	58
Figure 4.7: Plateau viscosity, $\mu_0$ , from fitted Bingham model to steady-state viscosity of aqueous 2 wt% HPMC E4M solution as a function of shear rate and griseofulvin concentration at 25°C .....	59
Figure 4.8: Adjusted yield stress, $\tau_y$ , from fitted Bingham model to aqueous 1 wt% HPMC E4M solution as a function of griseofulvin concentration at 25°C .....	59
Figure 4.9: Steady-state viscosity of aqueous 2 wt% HPMC E15LV solution as a function of shear rate and naproxen concentration at 25°C .....	61
Figure 4.10: Newtonian viscosity for aqueous 2 wt% HPMC E15LV solution as a function of naproxen concentration (un-sieved and various particle size ranges: > 125 micron, 75 to 125 micron, 45 to 75 micron and <45 micron) at 25°C .....	62
Figure 4.11: Plateau viscosity, $\mu_0$ , from fitted Bingham model to steady-state viscosity of aqueous 2 wt% HPMC E4M solution as a function of shear rate and naproxen concentration (un-sieved and various particle size ranges: > 125 micron, 75 to 125 micron, 45 to 75 micron and <45 micron) at 25°C ....	63
Figure 4.12: Adjusted yield stress, $\tau_y$ , from fitted Bingham model to aqueous 2 wt% HPMC E4M solution as a function of naproxen (un-sieved and various	

particle size ranges: > 125 micron, 75 to 125 micron, 45 to 75 micron and  
<45 micron) at 25°C ..... 64

## Chapter 1

### **Introduction**

In recent years there has been an increased interest in the development and commercialization of fast-dissolving edible films as a method for drug delivery. Overall, one of the most favorable routes of drug delivery is through oral ingestion due to its ease of administration, high patient compliance, cost-effectiveness, least sterility constraints, and flexibility in the design of the dosage form [1,2]. This has led to an increased interest and research by pharmaceutical companies in the reformulation of existing drugs into new dosage forms like fast-dissolving edible films [3]. Fast-dissolving oral delivery systems are solid dosage forms, which disintegrate within one minute when placed in the mouth without drinking or chewing [4]. This particular route of drug delivery addresses many patient compliance issues. For example, it is greatly favored by geriatric and pediatric patients alike, as it can overcome a patient's impediments in swallowing pills and their possible fears of choking [3,4].

Over the past few years, new developments on oral film strips have been achieved. Initially, oral film strips were developed for the oral care market as breath strips encountering great acceptance by consumers [5,6]. Nowadays, dissolvable oral thin films are an accepted technology for the delivery of active pharmaceutical ingredients (API) for over-the-counter (OTC) medications, and are being tested as a delivery method for prescription drugs [5]. Both consumers and pharmaceutical companies have accepted oral thin films as an alternative to traditional OTC medicine

forms, such as liquid solutions and dispersions, tablets, and capsules, as these offer a fast and accurate dosing, with the convenience of easy portability [3,5,7]. This drug delivery method also has its disadvantages as not all drugs can be incorporated into this type of dosage form. It is limited by the maximum deliverable dose, usually 50 mg or less [3,7,8]. Another challenge encountered with the production of these film strips is their oral bioavailability which depends on aqueous solubility, drug permeability, and dissolution rate, among other things [1].

Our research group has focused on the study of different biopolymers that can be used as a delivery system for pharmaceutical drugs. Previous studies have been performed on the properties of sodium alginate (NaAlg) and hydroxypropyl methylcellulose (HPMC) to determine if it can be used as a suspension medium for pharmaceutical drugs. NaAlg was used due to its wide use in the food and pharmaceutical industry as a thickener, immobilization agent, gelling agent, and to produce films and coatings, in addition to its lack of toxicity [7,9]. For NaAlg solutions, the existence of a thermotropic gelation was demonstrated through different rheological tests: constant-stress temperature-ramp, dynamic viscoelastic moduli, and thixotropy. For these solutions, silica was used as the model particle and it was demonstrated that the application of NaAlg as the film-forming medium with solid particles was limited [10].

In the case of HPMC solutions, the effect of surfactant and particle loading on the rheology and gelation of the solutions was studied. The model drug used was griseofulvin. This work showed that HPMC gelation temperature depends on the concentration and type of surfactant present in the solution. Additionally, gelation

temperature decreased in the presence of griseofulvin particles as these were promoting the formation of physical crosslinks [10,11].

A conventional method for the preparation of film strips is film casting, which requires a solvent evaporation step. Thus, it is important to understand the flow properties of the formulations as they are concentrated. For these reasons, the effect of BSC class II drug particle inclusions (drugs that are classified as having low solubility & high permeability [12]), griseofulvin and naproxen, in solutions of HPMC was studied by evaluating the change in viscosity at different shear rates as a function of particle loadings. The goal was to establish an empirical model that describes the viscosity as a function of HPMC concentration, drug concentration and size distribution, and shear rate. This will help us determine whether or not these conditions are favorable for the production of oral film strips.

## Chapter 2

### **Background**

As previously mentioned, there has been an increased interest in the development of fast dissolving oral film strips as a drug delivery method. Initially, these fast-dissolving oral film strips were available as breath strips, but their use has expanded into personal care, food and drug delivery [6]. Nowadays, the oral route is the most accepted and convenient way of administering pharmaceuticals. This is due to the fact that it has high patient compliance, cost-effectiveness, and flexibility in the design of the dosage form [1,2]. The additional advantages of dosing convenience and portability of oral strips has led to a wider acceptance by both pediatric and geriatric patients [3,5]. Recently, the main focus of pharmaceuticals and researchers alike has been on the development of film strips as an alternative method for drug delivery. Films have also gathered interest as an alternative to fast-dissolving tablets [4]. Geriatric and pediatric patients alike greatly favor this method as it can overcome patient's impediments in swallowing pills and their possible fears of choking [3,4]. Among the many advantages of oral strips are larger surface area for rapid disintegration and dissolution in the oral cavity, ease of transportation for consumer handling and storage, precision in the administered dose, ease of swallowing and no need for water, the dosage form can be consumed anywhere at anytime, increased bioavailability, and a reduction in the dose which means reduction in side effects associated with the medication [3].



Still, this drug delivery method also has disadvantages. Not all drugs can be incorporated into this dosage form, neither can it contain high doses of drugs as it has a maximum deliverable dosage [11], and poor bioavailability [1,3,7,8].

Biodegradable polymer gels have a wide variety of uses in many industries including agricultural, food, and pharmaceutical industries [13–15]. Biodegradable polymers are a reasonable alternative to formulate these films to transport solid pharmaceutical ingredients due to their gelling capacity, immobilization capacity in the gel network, and inherent flexible processing [7,13]. When selecting a polymer that fits these needs, natural biopolymers come to mind, as they are biodegradable and biocompatible. Many different materials have been considered for the development of these films. Among these are modified starches, gums, cellulose ethers, alginates, polyvinylalcohols, polyvinylpyrrolidines, or blends of these due to their film-forming properties [4]. Polysaccharides or natural polymers can be turned into hydrophilic matrices used for controlled release dosages [16].

## **2.1 Cellulose and its Derivatives**

Cellulose (Figure 2.1), a natural polysaccharide, is one of the most abundant naturally occurring substances [16–18]. Pure cellulose is insoluble in water due to the strong intramolecular and intermolecular interactions through hydrogen bonding [16–24]. The degree of polymerization of cellulose ranges from 1,000 to 15,000 glucose units [18]. Native cellulose is always polydisperse, meaning that it consists of a mixture of molecules with the same chemical composition but a wide range of average chain length [18]. The degree of substitution (DS) gives the average number of substituted hydroxyl

groups per anhydroglucose unit and has a value between 0 and 3, where 0 is for no substitution or native cellulose, and 3 for a completely substituted polymer [18,19,25]. Cellulose has many uses in various industrial applications, i.e. paper, paint, textile, food and pharmaceutical industries [18].

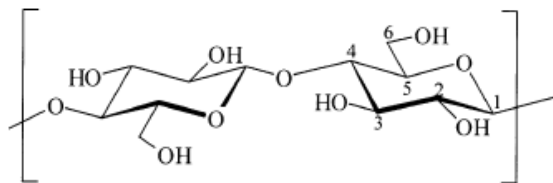


Figure 2.1: Structure of native cellulose. Reproduced from [19]

Among the available biopolymers, cellulose derivatives are of particular interest. Polymers based on cellulose have the potential of providing important functional properties and advantages that make them useful for industrial use since it is non-toxic, renewable, biodegradable, and modifiable [18,26]. Cellulose derivatives play an important role in many technical applications, especially in the pharmaceutical field where they have several uses, such as to modify the rheology of solutions and to control the release rate of drugs [27].

Cellulose derivatives are formed when different substituent groups replace the hydroxyl groups. As shown in Figure 2.2, the substitution of a fraction of the hydroxyl positions in each unit allows for the formation of water-soluble polymers with new properties [19,20]. The introduction of these substituents disturbs the inter- and intramolecular hydrogen bonds in cellulose, which leads to liberation of the hydrophilic character of the numerous hydroxyl groups and restriction of the chains to closely associate [18]. Substituents that disrupt the crystalline structure of cellulose increase the

solubility of the corresponding derivative [28]. Cellulose derivatives can be classified into two groups: cellulose esters and cellulose ethers. The difference among cellulose derivatives lies in the substitution of the hydroxyl groups in each anhydroglucose ring by other functional groups. Figure 2.3 shows two common cellulose derivatives, carboxymethyl cellulose (CMC) and hydroxypropyl cellulose (HPC), which shows the difference in the substituent groups of these derivatives.

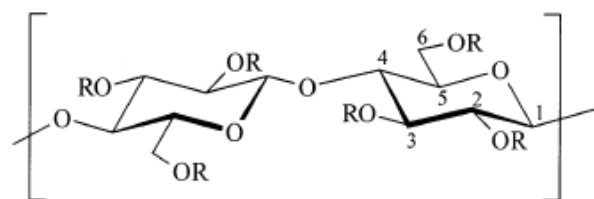


Figure 2.2: Structure of water-soluble cellulose derivatives (R=H or R from table 2.1 or 2.2). Reproduced from [19].

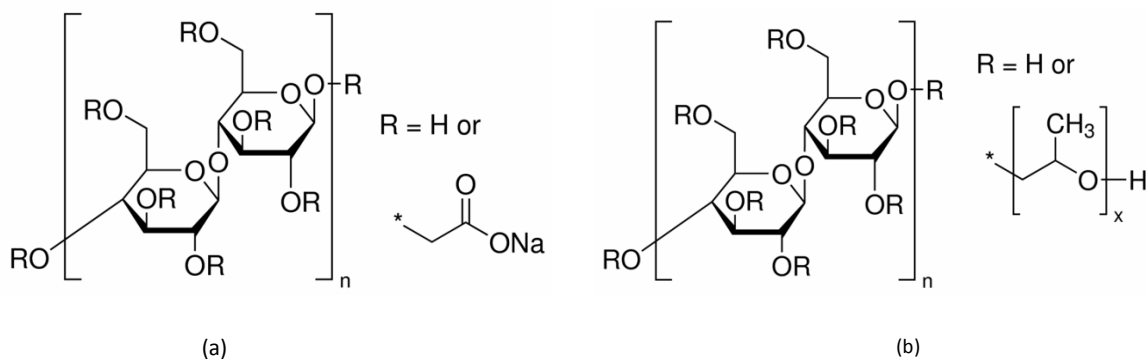


Figure 2.3: Cellulose derivative structures: (a) CMC and (b) HPC (reproduced from <http://www.sigmaaldrich.com>)

Tables 2.1, 2.2, and 2.3 list some of the most important water-soluble cellulose esters, ethers and mixed ethers, respectively. For instance, cellulose ethers are commonly used in the pharmaceutical industry as rate controlling agents for drug release. Therefore, they are found in various formulations like film coatings and tablet preparations [29].

Table 2.1: Substituents of water-soluble cellulose esters. Reproduced from [19]

Cellulose ester	-R
Cellulose acetat	-C(O)CH <sub>3</sub>
Cellulose xanthogenat	-C(S)SNa
Cellulose sulfat	-SO <sub>3</sub> Na
Cellulose phosphat	-P(O)(OH) <sub>2</sub>
Cellulose phthalat	-C(O)(C <sub>6</sub> H <sub>4</sub> )COONa

Table 2.2: Substituents of water-soluble cellulose ethers. Reproduced from [19]

Cellulose ether	-R
Carboxymethyl cellulose (CMC)	-CH <sub>2</sub> COONa
Sulfoethyl cellulose (SEC)	-CH <sub>2</sub> CH <sub>2</sub> SO <sub>3</sub> Na
Methyl cellulose (MC)	-CH <sub>3</sub>
Ethyl cellulose (EC)	-CH <sub>2</sub> CH <sub>3</sub>
Hydroxyethyl cellulose (HEC)	-CH <sub>2</sub> CH <sub>2</sub> OH
Hydroxypropyl cellulose (HPC)	-CH <sub>2</sub> CH <sub>2</sub> CH <sub>2</sub> OH
Cyanoethyl cellulose (CyEC)	-CH <sub>2</sub> CH <sub>2</sub> CN

Table 2.3: Substituents of water-soluble mixed ethers. Reproduced from [19]

Mixed cellulose ether	-R
Methylcarboxymethyl cellulose (MCMC)	-CH <sub>3</sub> , -CH <sub>2</sub> COONa
Hydroxyethylcarboxymethyl cellulose (HECMC)	-CH <sub>2</sub> CH <sub>2</sub> OH, -CH <sub>2</sub> COONa
Hydroxyethylmethylcarboxy methylcellulose (HEMCMC)	-CH <sub>2</sub> CH <sub>2</sub> OH, -CH <sub>3</sub> , -CH <sub>2</sub> COONa
Sulfoethylcarboxymethyl cellulose (SECMC)	-CH <sub>2</sub> CH <sub>2</sub> SO <sub>3</sub> Na, -CH <sub>2</sub> COONa
Hydroxyethylhydroxypropyl cellulose (HEHPC)	-CH <sub>2</sub> CH <sub>2</sub> OH, -CH <sub>2</sub> CH <sub>2</sub> CH <sub>2</sub> OH
Hydroxyethylmethyl cellulose (HEMC)	-CH <sub>2</sub> CH <sub>2</sub> OH, -CH <sub>3</sub>
Hydroxyethylethyl cellulose (HEEC)	-CH <sub>2</sub> CH <sub>2</sub> OH, -CH <sub>2</sub> CH <sub>3</sub>
Hydroxyethylpropyl cellulose (HPMC)	-CH <sub>2</sub> CH <sub>2</sub> OH, -CH <sub>2</sub> CH <sub>2</sub> CH <sub>3</sub>
Hydroxyethylsulfoethyl cellulose (HESEC)	-CH <sub>2</sub> CH <sub>2</sub> OH, -CH <sub>2</sub> CH <sub>2</sub> SO <sub>3</sub> Na

Modification leads to changes in the properties and behavior of the polymer, and consequently, optimization of attributes and characteristics [18]. Cellulose derivatives are biocompatible polymers and are mainly used in the food, pharmaceutical, and cosmetic industries for their properties as thickeners, binding agents, emulsifiers, film formers, suspension aids, surfactants, lubricants, and stabilizers [14,17–19,23,29–31].

In order to develop fast-dissolving films, the properties of the biopolymers and the effect of the desired deliverable drug need to be studied. In this case, the biopolymer of interest is hydroxypropyl methylcellulose (HPMC) (Figure 2.4). The effect on the viscosity of the polymer solutions with varying concentrations of drug particle inclusions at different shear rates will be studied. The drugs that will be used in this work are griseofulvin and naproxen, which are poorly soluble drugs and its chemical formulas are shown in Figure 2.5. Some of the drug properties are tabulated in Table 2.4 below.

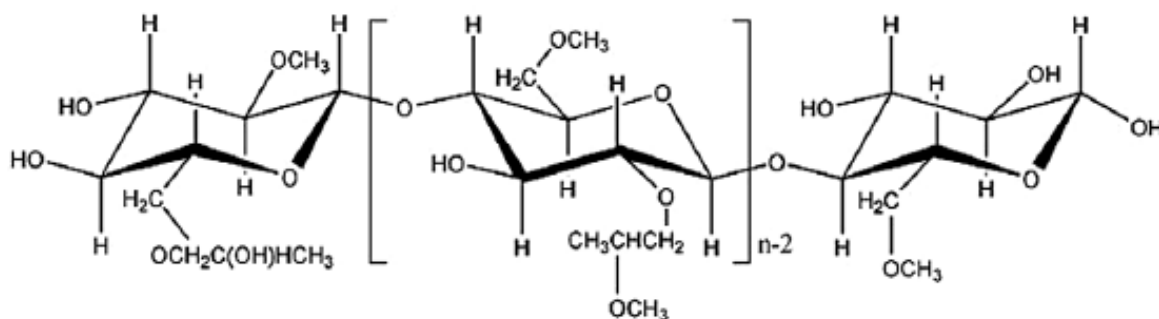


Figure 2.4: Chemical structure of hydroxypropyl methylcellulose. Reproduced from [17].

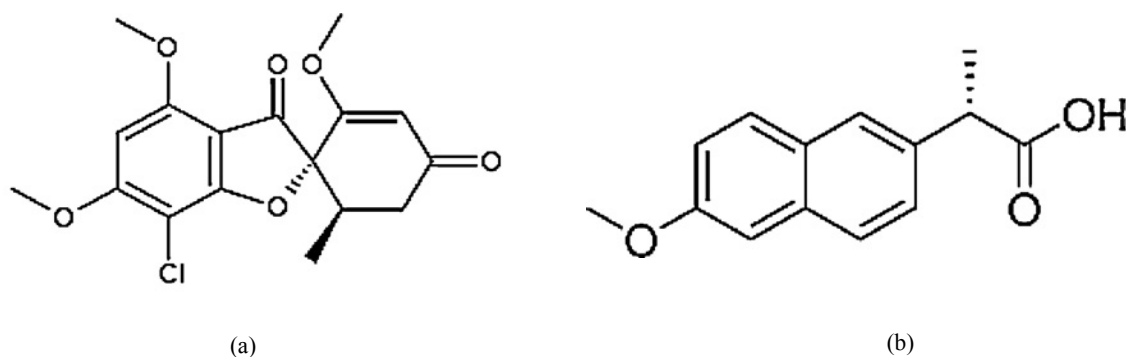


Figure 2.5: Chemical Structure of drug molecules: (a) griseofulvin and (b) naproxen. Reproduced from [32]

Table 2.4: Physicochemical properties of the drugs. Reproduced from [32]

Drug	Solubility (in H <sub>2</sub> O, mg/L)	Molecular weight	Melting point (°C)
griseofulvin	8.99	352.8	220.0
naproxen	17	230.26	153

Polymer films have an advantage over other forms of oral drug delivery for poorly soluble drugs because they provide a larger surface area which leads to rapid disintegration and dissolution in the oral cavity [32]. One of the things that needs to be analyzed before proceeding to prepare these films is the drug content that can be carried in it, determine if the drug is distributed homogeneously along the film, and the effect the drug particles have on the properties of the film. The first step is to determine the effect the drug has on the polymer in order to determine whether or not it is a suitable carrier for the particular drug and maximum loading. Since the interactions between the drug molecules and polymer can produce differences in the film properties, they need to be identified for product development.

## 2.2 Hydroxypropyl methylcellulose

HPMC is one of the most important hydrophilic carrier materials used for the preparation of oral controlled drug delivery systems [22,33–40]. Among the many reasons for the use of HPMC as an excipient are that it is water-soluble [16,22,36,41], nontoxic, easy to handle, relatively cheap, easy to compact, able to accommodate high levels of drug loading [34,36,38–41], efficient thickener, film forming ability, and capacity to form thermal gels that melt upon cooling [10,16,40]. HPMC is a traditional gel former in hydrophilic matrix tablets and the release of the drug from these matrixes

composed of it depend on the degree of substitution and molecular weight of the polymer [28,36]. Figure 2.4 shows the structure of HPMC, where the R group represents a  $-\text{CH}_3$ ,  $-\text{CH}_2\text{CH}(\text{CH}_3)\text{OH}$  group or a hydrogen atom.

The degree of substitution of HPMC, the hydroxypropyl and methoxy group content, and its molecular weight greatly influences the chemical properties of this polymer [16,22,28,33,38,40,42–44]. The degree of substitution (DS) defines the average number of hydroxyl groups per anhydroglucose unit where hydrogen is replaced by methyl and molar substitution (MS) represents the average number of propylene oxide groups per anhydroglucose unit [45]. Along the cellulose backbone, methyl substitutes constitute hydrophobic zones whereas hydroxypropyl groups are more hydrophilic [40,45]. The molecular weight of HPMC plays a dominant role in changing the viscosity when the polymers have similar chemical structures [38]. The U.S. Pharmacopeia Convention (USP) identifies four different types of HPMC depending on their hydroxypropoxy and methoxy content: HPMC 1828, HPMC 2208, HPMC 2906, and HPMC 2910 [33]. In this type of classification, the first two numbers indicate the percentage of methoxy groups and the last two indicate the percentage of hydroxypropoxy groups. Table 2.5 shows the differences among the substitution degree of the different substituent groups in the four classes of HPMC. Typical representatives of USP 2208 and USP 2910 are Methocel K4M and E4M, which contain respectively 22.5% methoxy and 9.2% hydroxypropyl, and 29.5% methoxy and 9.3% hydroxypropyl [35]. HPMC is also known as Methocel which is classified by a letter (K, E or F) followed by a number and a letter afterwards. In this method of identification, the first letter identifies the chemistry of the type of cellulose ether. The number that follows the

initial letter identifies the viscosity grade in mPa-s for the product measured in 2% aqueous solution at 20 °C. The letter following the number identifies the viscosity, i.e. the letter ‘M’ suggests the value a factor of 1000 and the abbreviation ‘LV’ represents a special low viscosity product series [15]. Table 2.6 below shows the methoxy and hydroxypropoxy content on each HPMC type when using this nomenclature

Table 2.5: USP specification for different type of HPMC, classified according to their degree of methoxy and hydroxypropyl substitution. Reproduced from [33].

Substitution Type	Methoxy (%)		Hydroxypropoxy (%)	
	Min.	Max.	Min.	Max.
1828	16.5	20.0	23.0	32.0
2208	19.0	24.0	4.0	12.0
2906	27.0	30.0	4.0	7.5
2910	28.0	30.0	7.0	12.0

Table 2.6: Various grades of HPMC. Reproduced from [15].

HPMC type*	Methoxy (%)	Hydroxypropoxy (%)	Also known as:
K	19-24	4-12	Hypromellose 2208
E	28-30	7-12	Hypromellose 2910
F	27-30	4-7.5	Hypromellose 2906

\*Different viscosity grades available on the market [15]

The properties of the HPMC solutions, like viscosity, gelling capacity, gelation, and temperature, among others, depend on the molar mass and degree of substitution of the HPMC [41,44]. Different solubilities of this polymer are attributed to the amount of the two substituents present [29,41]. Overall, the degree of substitution influences the pharmaceutical relevant properties, like gelling capacity, flowability, and release rate, of HPMC [29]. Additionally, temperature influences the intermolecular interactions (i.e. cloud point), gelation, drug release rates, and viscoelastic properties of the gel [44].



The molecular structure and conformation of the polymer in solution is very important for the flow behavior, which in turn is important for several processes in pharmaceutical and other industries [34,43]. The conformation and structure of a polymer in solution is influenced by the chemical structure, the molar mass, concentration, temperature and the solvent used. The formation of intermolecular hydrogen bonding between hydroxyl groups of HPMC chains and water molecules as well as water cages surrounding hydrophobic clusters of HPMC chains such as methoxyl substituted and relatively less hydrophobic hydroxypropyl substituted regions makes HPMC soluble at low temperature [38]. Water cages are defined as the formation of water-water hydrogen bonding in the hydrophobic hydration shell [38].

Haque and co-workers studied the effect of hydroxypropyl substituents on the thermogelation of methylcellulose [46]. For this particular study, they used methylcellulose (A4M) and three different hydroxypropylmethyl derivatives labeled ‘E’, ‘F’ and ‘K’ containing different percentages of substitution (Table 2.7). In the HPMCs used, the methyl groups remained the dominant substituent but they also contained smaller amounts of the larger more polar hydroxypropyl group [46].

Table 2.7: Composition for Methocel cellulose derivatives used by Haque and Morris [46].

Material	Average number of substituents per residue	
	Methoxyl	Hydroxypropyl
A4M	1.6-1.9	0
E4M	1.8-2.0	0.20-0.31
F4M	1.7-1.9	0.10-0.20
K4M	1.1-1.6	0.10-0.30

When Haque and coworkers [46] performed a differential scanning calorimetry (DSC) analysis (Figure 2.6), they observed that all three HPMC types show a single endotherm on heating and a single exotherm on cooling, with substantial thermal hysteresis. The cooling exotherms for the HPMCs span approximately the same range of temperature (from 70 to 45°C) and are comparable in width to the first exothermic process observed for methylcellulose, but displaced to higher temperature. Haque and coworkers attributed these peaks to the heat released by the formation of water cages around hydrophobic substituents exposed to the aqueous environment on dissociation of the gel network. Additionally, the second exotherm observed for methylcellulose, which is attributed to enthalpic interactions with cellulosic bundles is not seen for the other samples. This indicates that the hydroxypropyl substituents cause a reduction in the enthalpic stability of the bundles [46].

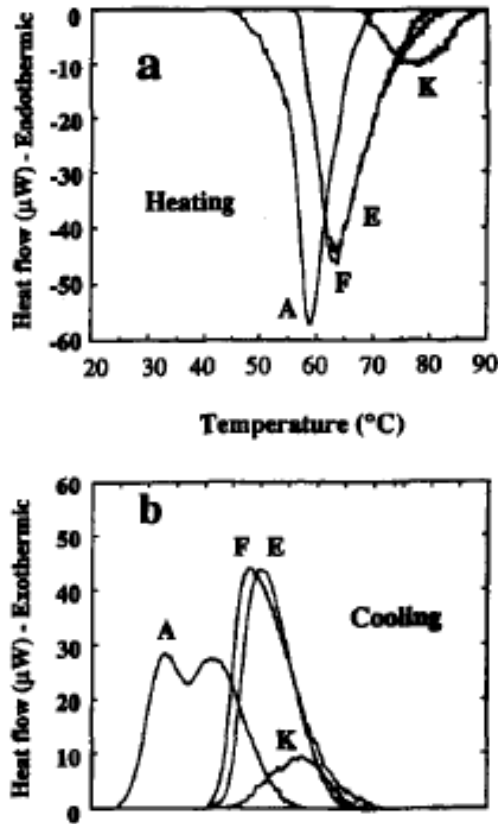


Figure 2.6: DSC traces for 2% (w/v) methylcellulose and HPMC from Haque and Morris on (a) heating and (b) cooling at  $0.1 \text{ deg min}^{-1}$ . Reproduced from [46].

A known way of determining the interactions in a solution is by comparing steady-shear viscosity ( $\eta$ ) from large deformation measurements with the dynamic viscosity ( $\eta^*$ ) from small deformation measurements using low-amplitude oscillation [47]. When performing rheological studies of the various HPMC's, Haque and coworkers observed that the shear-rate dependence of steady-shear viscosity ( $\eta$ ) and frequency dependence of complex dynamic viscosity ( $\eta^*$ ) superimpose closely. This demonstrates the lack of enthalpic interactions between the individual species present in the solution.

The shear-rate dependence of viscosity for underivited polysaccharide coils can be fitted to the relationship:

$$\eta = \eta_0 - \left[ \left( \frac{1}{\dot{\gamma}_{1/2}} \right)^p \right] \eta \dot{\gamma}^p \quad (2.1)$$

where,  $\eta_0$  is the maximum Newtonian viscosity at low shear rate,  $\dot{\gamma}_{1/2}$  is the shear rate at which  $\eta = \eta_0/2$ , and  $p$  has a constant empirical value of 0.76 [46]; giving a linear relationship on plots of  $\eta$  vs.  $\eta \dot{\gamma}_{1/2}$ . For HPMC, the plots show curvature for values of  $p = 0.76$  (Figure 2.7a) but shows a linear relationship at  $p = 0.56$  for methylcellulose (Figure 2.7b) [46]. When looking at all the HPMC samples, they all show an identical form of shear thinning, leading the researchers to conclude that, as with methylcellulose, the bundle structure proposed is also present in the solutions of HPMC (Figure 2.8).

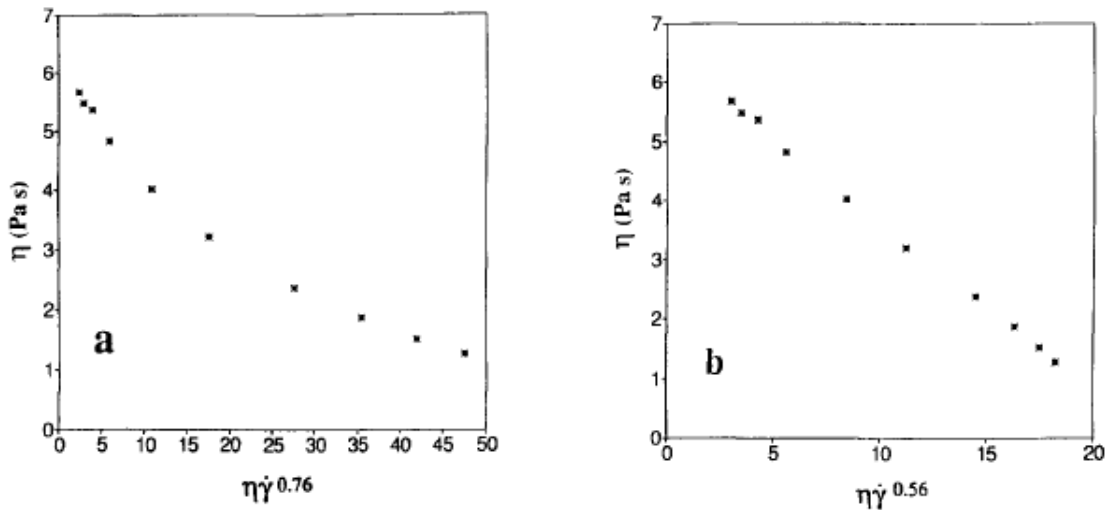


Figure 2.7: Shear thinning behavior of 2% (w/v) E4M plotted as  $\eta$  vs.  $\eta \dot{\gamma}^p$  for (a)  $p=0.76$  and (b)  $p=0.56$ . Reproduced from [46].

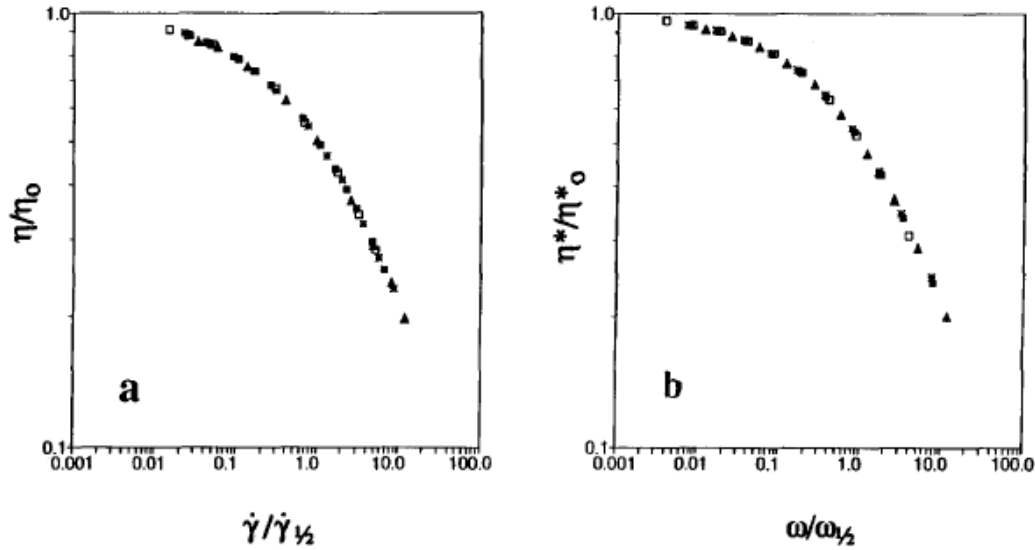


Figure 2.8: Generalized shear thinning behavior of Methocel samples A4M (n), E4M ( $\Delta$ ), F4M ( $\square$ ) and K4M (\*); (a) steady-shear viscosity; (b) complex dynamic viscosity;  $\eta = \eta_0/2$  at  $\dot{\gamma} = \dot{\gamma}_{1/2}$ ;  $\eta^* = \eta^*_0/2$  at  $\omega = \omega_{1/2}$ . Reproduced from [46].

Hussain and co-workers focused their work on the thermoreversible gelation of cellulose derivatives like methylcellulose (MC) and HPMC [25]. They focused on describing the use of rheology as a method to study the thermal transitions of various HPMC solutions, particularly the effects of temperature on concentrated systems of up to 20% w/w [25]. Hussain et al. used a particular type of HPMC to perform their tests; HPMC E4M, which has 28-30% methoxy substituents and 7-12% hydroxypropyl substituents (equivalent to USP HPMC type 2910; see Table 2.5). Their results are presented in Figure 2.9 below. For the solution of 2% w/v, at 20 °C,  $G''$  was observed to be greater than  $G'$  which indicates that the viscoelastic system is dominated by the liquid component [25]. For the 20% w/v HPMC solution, when the solution was heated,  $G'$  dropped sharply at 60 °C and rose at 65 °C, while  $G''$  fell sharply at 55 °C and leveled off

at 65 °C. When cooling,  $G'$  increased below 65 °C and leveled off to 50 °C while,  $G''$  rose sharply above 70 °C and leveled off below 50 °C.

In addition, Hussain and co-workers performed frequency sweeps (Figure 2.10) at different temperatures for a 12% solution of HPMC. At a temperature of 25 °C, both  $G'$  and  $G''$  showed a marked increase with frequency. At 55 °C, the frequency dependence decreased and when a temperature of 85 °C was reached, the frequency dependence decreased even more. This low frequency dependence is characteristic of a polymer gel [25]. The general behavior is that at low temperatures the indices are relatively high, which indicates a viscous system, while at higher temperature the frequency dependence is considerably reduced, which in turn reflects the more elastic nature of the gelled system [25].

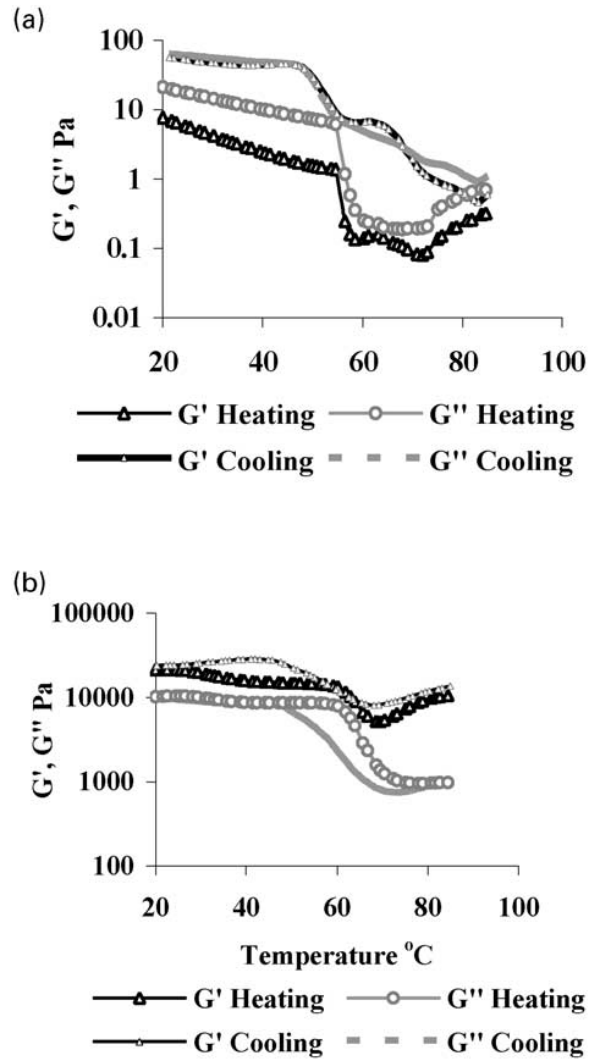


Figure 2.9: Thermorheogram of a 2% (w/v) (a) and 20% w/v (b) HPMC E4M system. Reproduced from [25].

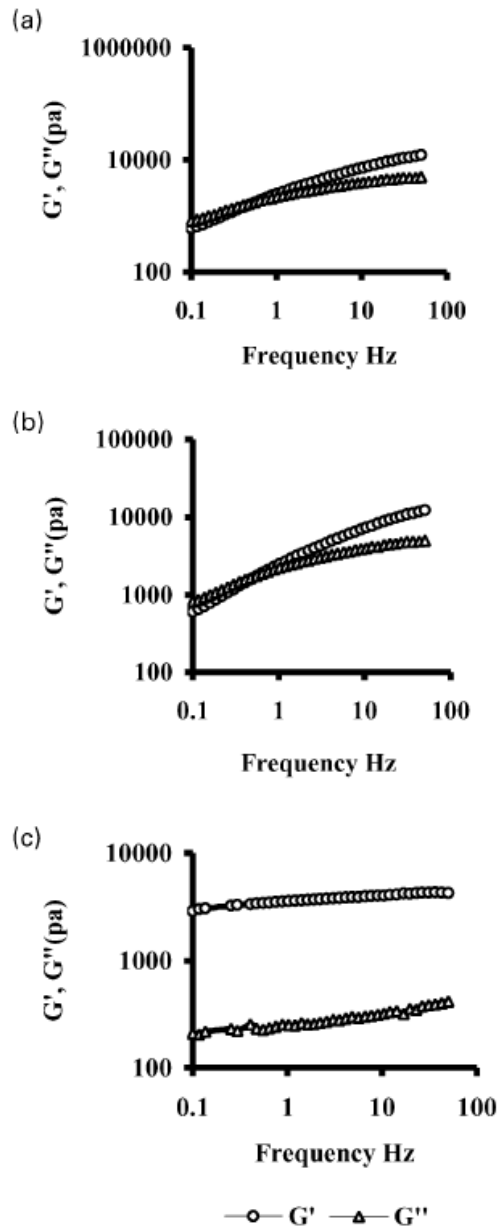


Figure 2.10: Frequency sweeps of 2% E4M solutions at 25 (a), 55 (b) and 85°C (c). Reproduced from [25].

Silva and co-workers performed oscillatory tests to study the effect of temperature on the gelation of HPMC solutions (Figure 2.11) [17]. It was observed that, in general, as the temperature of the sample was increased,  $G''$  decreased until it reached a



characteristic temperature. After this temperature was reached, a marked decrease was observed. A similar behavior was observed for  $G'$ , but the final decrease was less accentuated when compared to  $G''$  and it was not observed for the 1% solution. The characteristic temperature seen throughout all the samples was slightly above 70 °C, independent of the concentration of HPMC. Silva and co-workers observed that there was a final increase in both moduli with increasing temperature but it was more significant for the storage modulus over the loss modulus, which was where  $G'$  and  $G''$  curves intersect. The point where the moduli crossed depends on the polymer concentration and on the frequency applied when conducting the oscillatory tests [17].

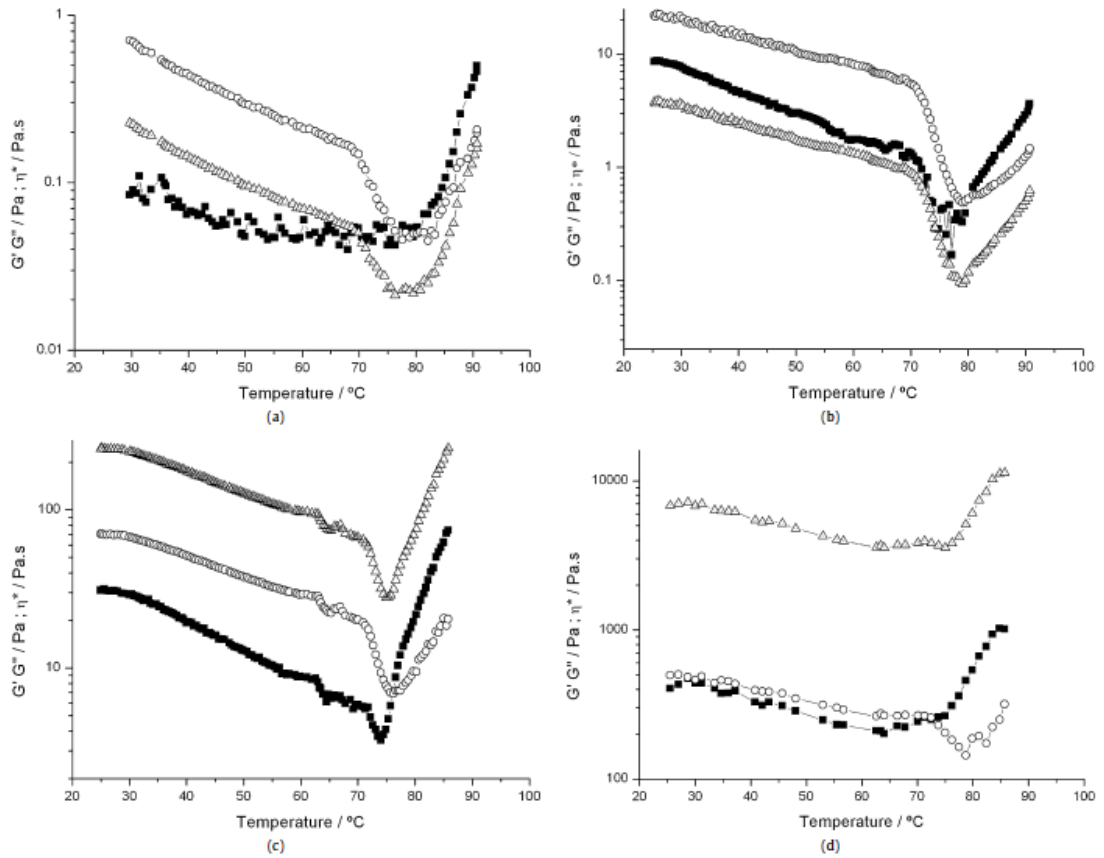


Figure 2.11: Storage ( $G'$ , squares), loss ( $G''$ , circles) and the complex viscosity ( $\eta^*$ , triangles) modulus, as a function of temperature, for HPMC solutions of (a) 1%, (b) 2%, (c) 5% and (d) 10% w/w. Frequency is chosen so as to impose a value of  $G''$  higher than  $G'$  at the initial conditions. Reproduced from [17].

Solutions of HPMC in water exhibit the phenomenon of thermoreversible gelation, i.e. gels on heating and re-dissolves on cooling [48]. Ford established that the gelation depends on the degree of total substitution and degree of hydroxypropyl substitution [48]. The gelation of HPMC depends strongly on the molar substitution of the hydroxypropyl groups. Figure 2.12 below shows two inflection points for HPMC.

As the temperature was increased, the  $G'$  and  $G''$  values decreased until a temperature was reached where the values decreased sharply. As the temperature continued to increase, the solutions began to gel and both  $G'$  and  $G''$  values increased. The gel strengths of HPMC solutions increased with increases in DS and decreases in MS [48].

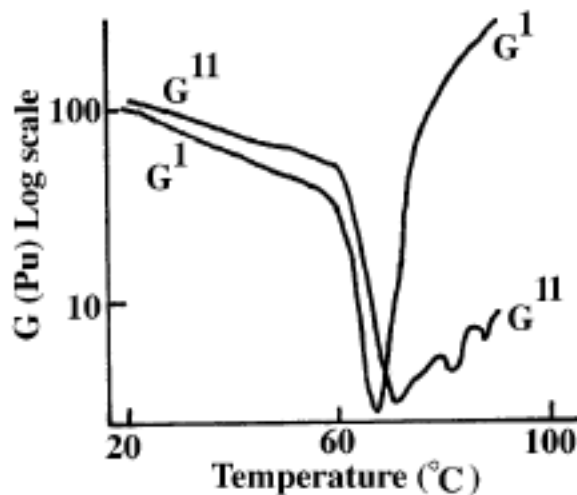


Figure 2.12: The influence of temperature on the  $G'$  and  $G''$  values for a 4% solution of a 4000 mPa viscosity grade HPMC polymer with DS of 1.85 and MS of 0.16 at a frequency of 1 Hz and 8.5 % amplitude heated at a scan rate of 1 C min<sup>-1</sup>. Reproduced from [48].

Camino et al. studied the gelation of HPMC and agreed with the prepared two-step mechanism for gelation process where the first step is the pre-gel regime which is then followed by the gel regime [45]. The first step involves hydrophobic interactions that lead to cluster formation of broad shapes and sizes. It is during this stage that a transition from a clear to a turbid solution was observed (cloud point). The gel regime corresponds to the gelation that occurs at a higher temperature. At this point, phase separation can occur [45].

Perez et al. performed dynamic rheometry studies to determine the gel point of HPMC. Figure 2.13 shows the storage and loss moduli for a 6% HPMC solution. A strong decrease in  $G'$  (storage modulus) was observed related to the dehydration of cellulose chains leading to an increase in the interactions of the hydrophobic groups [40]. The gelation temperature was found to be the temperature where a fast increase in  $G'$  values was observed which was around  $60^\circ\text{C}$ . An increase in  $G'$  was observed up to  $75^\circ\text{C}$ , where the maximum HPMC gel development took place. Above  $75^\circ\text{C}$ ,  $G'$  slowly increased which was attributed to a phase separation.

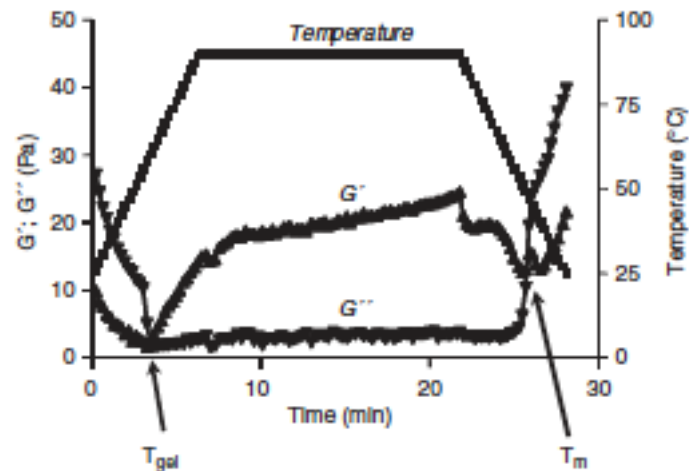


Figure 2.13: Evolution of elastic ( $G'$ ) and viscosu ( $G''$ ) moduli upon heating and cooling HPMC solution (pH 7).  $T_{gel}$ : gelation temperature;  $T_m$ : melting temperature. Reproduced from [40]

Low viscosity HPMCs are widely used in film-forming applications, which might be influenced by the drug particle interactions affecting the properties of the desired applications. Drug-polymer interactions can affect the viscosity and the

strength of the gel layer, therefore changing the mechanical and diffusion barrier properties which affect the drug release kinetics.

For HPMC, the distribution of substituents is heterogeneous as a result of the manufacturing process, and the heterogeneous distribution of methoxyl moieties appears to be crucial for the thermal gelation process. The extent of methoxyl and hydroxypropyl substitution markedly affects the sol:gel transition temperature [20]. Bajwa and co-workers studied the thermal gelation process of HPMC in order to relate these to the rheological changes in aqueous HPMC solutions during the sol:gel transition [20]. The HPMC used in this work contained 9.3% hydroxypropyl and 29.5% methoxyl substituents. Figure 2.14a shows the viscoelastic moduli and  $\tan \delta$  values for a 2% w/w HPMC solution during the heating cycle. Raising the temperature from 10 °C resulted in a decrease of the storage modulus ( $G'$ ) around 43 °C. This was followed by an increase in  $G'$ . The reduction in  $G'$  was attributed to a progressive disruption of native cellulosic bundles, while the increase was attributed to the unbundling of the constituent strands of polymer at the ends of the bundles, followed by the formation of a network of swollen clusters [20]. A sharp decrease was observed at 56 °C for the loss modulus ( $G''$ ), which was attributed to the high molecular weight fractions of polymer precipitating from solution [20]. The gelation process began at the point where  $\delta = 1$  ( $G' > G''$ ), the point where the polymer solution exhibits a change from a liquid-like to a solid-like system [20].

Figure 2.14b shows the viscoelastic moduli and  $\tan \delta$  values for a 2% w/w HPMC solution during the cooling cycle. A significant hysteresis was observed upon

cooling, which suggested that the dissociation of aggregated cellulosic bundles occurs at a higher temperature than when they re-form on cooling [20,47].

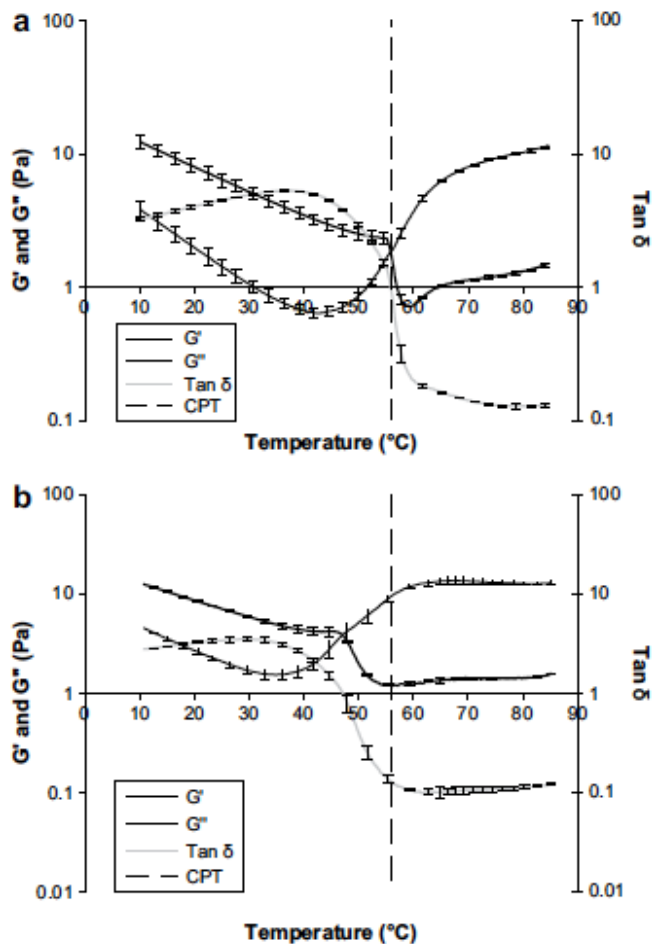


Figure 2.14: The effect of temperature on the viscoelastic moduli and  $\tan \delta$  of 2% w/w HPMC solutions during (a) heating and (b) cooling cycles. Reproduced from [20].

Kawaguchi and Ryo studied the rheological properties of silica suspensions in HPMC solutions as a function of silica concentration and different molecular weights of HPMC [49]. The HPMC concentrations ranged from 0.5 to 2.5 % and silica content in the silica suspensions were 2.5, 5.0 and 7.5 %. A shear thinning behavior

was observed for all the HPMC solutions used. When the storage ( $G'$ ) and loss ( $G''$ ) moduli were evaluated, it was observed that both moduli values increased with an increase in HPMC concentration. For 2.5 and 5.0 % silica suspensions a value where  $G''$  exceeds  $G'$ , signifying the change in the structure of the silica suspension from viscoelastic solid-like to viscoelastic liquid-like matter with increasing frequency was found. Yet, for higher concentration of 7.5 wt%, the crossover between  $G'$  and  $G''$  was not observed. This indicated a viscoelastic solid behavior [49]. They concluded that the rheological properties depend on the silica content present in the solution.

Acevedo et al studied the thermal gelation of aqueous HPMC solutions with sodium dodecyl sulfate (SDS) and hydrophobic drug particles [11]. The viscosity of a solution can provide information about conformational effects caused by polymer-surfactant interactions. The steady-state viscosity of aqueous HPMC solutions showed a Newtonian plateau at low shear rates (below  $10 \text{ s}^{-1}$ ) followed by a shear thinning regime at higher shear rates. Figure 2.15 shows the gelation temperature ( $T_{\text{gel}}$ ) of HPMC systems as a function of SDS concentration with and without griseofulvin. The gelation temperature for pure HPMC was reported as  $57.4 \pm 1.5 \text{ }^\circ\text{C}$ . The addition of SDS at low concentrations did not affect greatly the  $T_{\text{gel}}$  for HPMC without griseofulvin. At 5.0 mM a drop of  $5.6 \text{ }^\circ\text{C}$  in  $T_{\text{gel}}$  relative to that of pure HPMC is observed. As the concentration of SDS is increased,  $T_{\text{gel}}$  increases to  $61.0 \text{ }^\circ\text{C}$ . Additionally, it can be observed that the initial addition of griseofulvin drug particles, in the absence of SDS, decreases the  $T_{\text{gel}}$  of the HPMC solution.

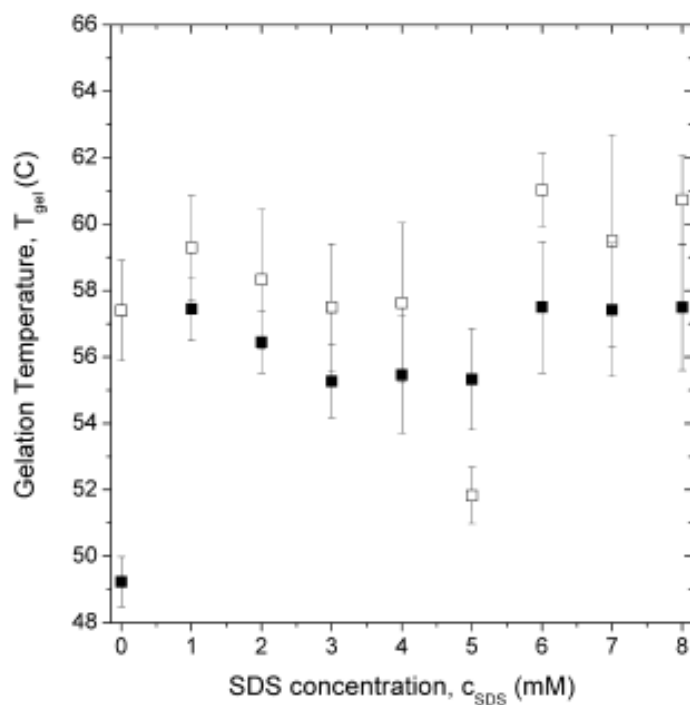


Figure 2.15: Gelation temperature of 1 wt% aqueous HPMC solutions as a function of SDS concentration in the absence (□) or presence (■) of 1 wt% griseofulvin. Reproduced from [11].

The effect of SDS on the magnitude of zero-shear steady-state viscosities of HPMC solutions at 25 °C was also measured (Figure 2.16). At concentrations below 4 mM of SDS no significant effect on viscosity was observed. Above 5.0 mM, the viscosity increased by up to a factor of two, which was attributed to the formation of aggregates. With the addition of griseofulvin particles, a decrease in viscosity in the absence of SDS was observed which was due to the adsorption of the polymer on the drug particles' surface.



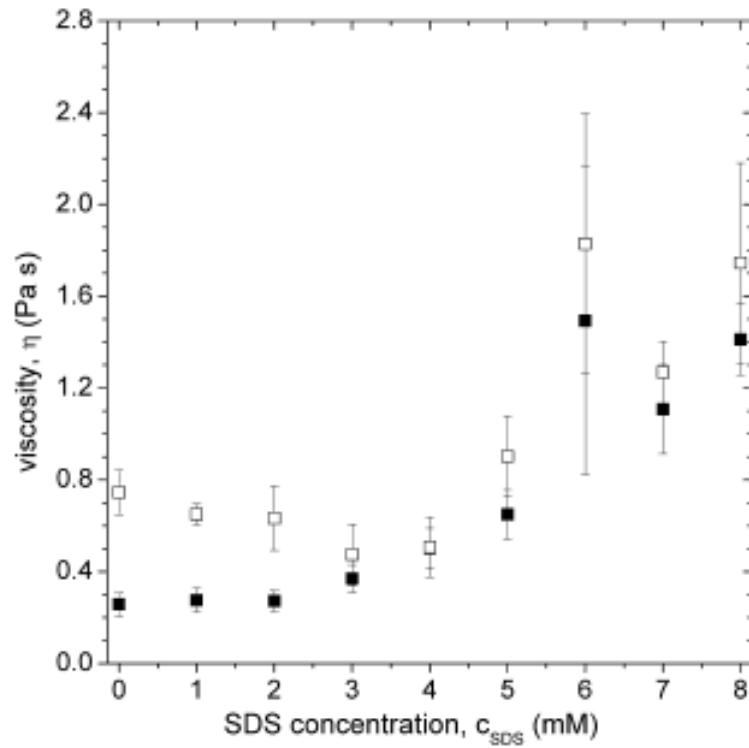


Figure 2.16: Zero-shear steady state viscosity of aqueous HPMC solutions at 1 wt% with SDS in the absence ( $\square$ ) or presence ( $\blacksquare$ ) of 1 wt% griseofulvin. Reproduced from [11].

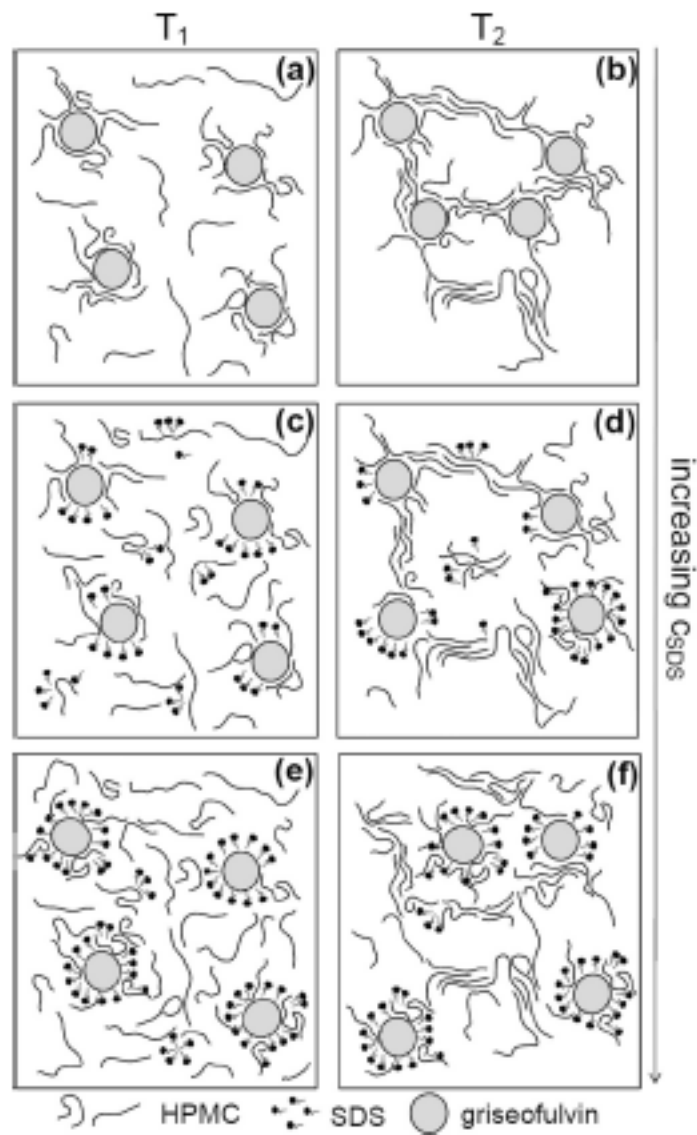


Figure 2.17: Schematic representation showing the interactions between HPMC, SDS, and griseofulvin at  $T_1$  and  $T_2$ , where  $T_1 < T_{gel} < T_2$ . Panes (a) and (b) represent the system with no SDS; panes (c) and (d) represent the system with limited concentration of SDS; and panels (e) and (f) represent the system with higher concentration of SDS, but below the critical micelle concentration. Reproduced from [11].

Figure 2.17 shows a schematic representation of the proposed mechanism for HPMC gelation in the presence of SDS with and without griseofulvin at temperature below

( $T_1$ ) and above gelation ( $T_2$ ). According to their proposed mechanism, the gelation process is mainly affected by two competing processes: griseofulvin acting as a binding agent of associated hydrophobic polymer regions which include adsorbed polymers and polymer-surfactant complexes, and SDS aggregating with the HPMC through hydrophobic interactions. At a temperature below  $T_{gel}$  and in the absence of SDS (Figure 2.17a), some HPMC binds to the surface of the particles. The particles with adsorbed polymer help to bridge hydrophobic regions during the gelation (Figure 2.17b). With the addition of SDS at low temperature (Figure 2.17c), some of the adsorbed HPMC is replaced with SDS and forms polymer-surfactant interactions. SDS is shown to decrease bridging effects at both temperatures (Figure 2.17d). At higher concentrations of SDS (Figure 2.17e), the HPMC is free in solution and complexed with the bound SDS. As the temperature is increased, the opposing effects mostly cancel each other. The decrease in viscosity due to the addition of drugs to HPMC demonstrates that HPMC adsorbs on the particles surface. Hydrophobic interactions between adsorbed polymer on griseofulvin and free polymer in solution during gelation account for the synergistic effect on gel transition. As the concentration of SDS increased, it suggests that the polymeric chains are saturated and larger surfactant aggregates account for the increase in viscosity.

Silva et. al. studied the change in viscosity of HPMC with temperature at different values of shear rate (Figure 2.18) [17]. They observed that for lower shear rates, the Newtonian viscosity decreased as the temperature rose until it reached the gelation temperature, which depends on the concentration of the polymer. After this

point, a sharp increase in the viscosity was observed. For the higher values of shear rate (i.e. non-Newtonian regime), the viscosity suddenly dropped close to the temperature at which the gelation occurs.

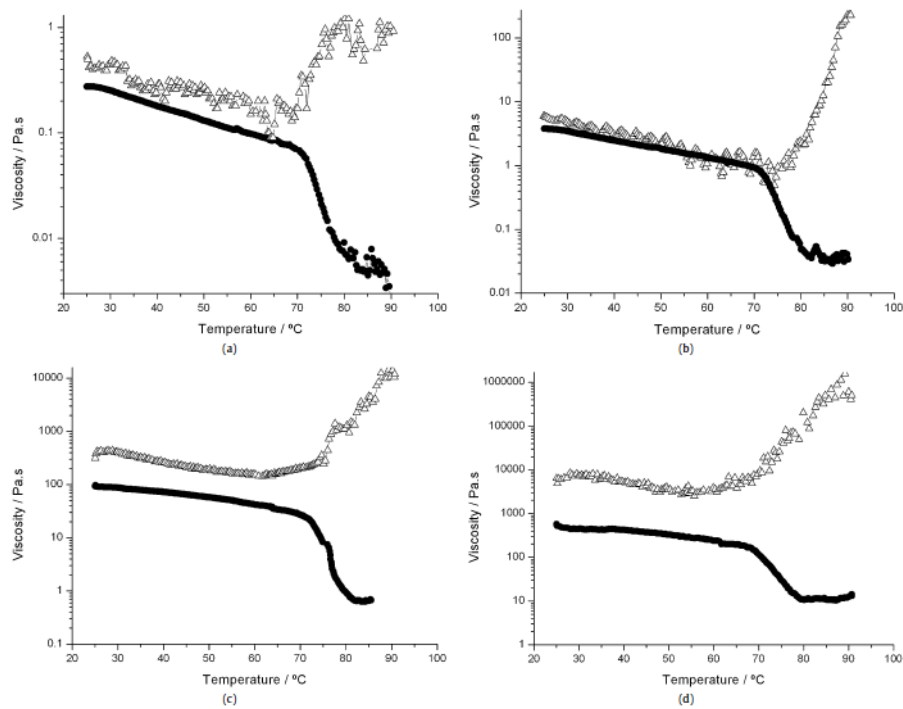


Figure 2.18: Viscosity dependence on temperature for HPMC solutions of (a) 1%, (b) 2%, (c) 5% and (d) 10%, w/w. Curves are obtained at Newtonian shear rates (triangles), with imposed values respectively of  $0.5$ ,  $0.05$ ,  $5.0 \times 10^{-3}$  and  $1.0 \times 10^{-3} \text{ s}^{-1}$ , and non-Newtonian shear rates (circles, of  $50$ ,  $30$ ,  $5$  and  $1 \text{ s}^{-1}$  respectively. Reproduced from [17].

By measuring viscosity versus temperature plots for various values of shear rates, Silva and coworkers were able to observe that when the shear rate is increased the point at which the viscosity starts to increase moved to higher temperatures.

Additionally, for temperatures below the gelation temperature, the effect of shear rate upon viscosity was limited. It was observed that as temperature increases, the viscosity decreased but the Newtonian regime remained unaffected. For temperatures above 70 °C, a shear thinning behavior was observed. In general, low shear rates correspond to high viscosities, which decreased sharply when a large enough shear rate was applied to it.

Viriden and co-workers studied the viscosity of different batches of HPMC (Table 2.8). The apparent viscosity was found to decrease with increasing shear rates in the two 90SH100 batches, which implies that these solutions were shear thinning. The two batches of 0.050 Pa-s viscosity grade showed a Newtonian behavior within the studied interval of shear rates [39].

Table 2.8: HPMC batches and their properties. Reproduced from [39]

<b>Grade</b>	<b>Hydroxypropyl content</b>	<b>Methoxyl Content</b>
60SH50	9.0	29
65SH50	6.3	27.7
90SH100SR	9.2	22.6
90SH100	5.6	23.8

Fatimi et al. studied the dependence of the steady shear viscosity on the shear rate of HPMC at concentrations ranging from 1% to 5% in NaOH (0.2M) at 25°C. HPMC E4M with a 1.9 methoxyl degree of substitution (29.% methoxyl) and 0.23 hydroxypropyl molar substitution (9.7% hydroxypropyl) was used. A Newtonian plateau at low shear rates followed by a shear thinning behavior was observed [26]. At

high shear rate values, a power-law dependence with shear rate was observed on the viscosity. The flow curves were fitted using the simplified Cross model:

$$\eta = \frac{\eta_0}{1 + (\lambda\dot{\gamma})^n}$$

where  $\eta_0$  is the limiting Newtonian viscosity at low shear,  $\lambda$  is the relaxation time (the inverse of a critical shear rate  $\dot{\gamma}_c$ ), and  $n$  is the exponent of the power law. Table 2.9 lists the parameter values at the different concentrations for the HPMC solutions.

Table 2.9: Values of Cross parameters at different concentrations for HPMC solutions at 25°C. Reproduced from [26].

Polymer	$c$ (% w/w)	$\eta_0$ (Pa s)	$\lambda$ (ms)	$n$	$\dot{\gamma}_c$ (s <sup>-1</sup> )
HPMC	1.0	0.010 ± 0.000	0.031 ± 0.004	0.831 ± 0.099	–
	1.5	0.043 ± 0.001	0.273 ± 0.004	0.830 ± 0.012	3668.00 ± 58.64
	2.0	0.073 ± 0.002	0.430 ± 0.024	0.786 ± 0.013	2328.33 ± 129.62
	2.5	0.260 ± 0.008	1.314 ± 0.011	0.742 ± 0.014	760.80 ± 6.68
	3.0	0.811 ± 0.013	3.062 ± 0.088	0.740 ± 0.000	326.73 ± 9.52
	3.5	1.571 ± 0.041	5.511 ± 0.323	0.773 ± 0.008	181.87 ± 10.90
	4.0	2.435 ± 0.054	8.069 ± 0.523	0.768 ± 0.006	124.27 ± 7.84
	4.5	4.409 ± 0.079	14.002 ± 0.803	0.777 ± 0.015	71.58 ± 4.20
	5.0	6.636 ± 0.880	18.641 ± 1.454	0.780 ± 0.020	53.86 ± 4.18

The limiting Newtonian viscosity was observed to increase with increasing polymer concentration and the Newtonian plateau limit shifted to a lower shear rate region [26].

Various works have suggested that individual drugs can change the physicochemical properties of non-ionic cellulose ethers in solutions, gels and matrices [50]. This was the focus of the study performed by Pygall and coworkers with HPMC Methocel E4M CR Premium USP 2910 having a 9.3% hydroxypropyl and 29.5% methoxyl substitution, and a nominal viscosity of 4000 cps for a 1% (w/w)

solution at 20 °C and two drugs, diclofenac sodium and meclofenamate sodium. Figure 2.19 shows the viscosity profiles for 1% (w/w) HPMC solutions at 20 °C, as a function of shear rate (0.01-100 s<sup>-1</sup>) at various drug concentrations. A Newtonian plateau at low shear rates and a tendency to shear thin at high shear rates was observed for the HPMC solutions with no drug. The inclusion of 10 and 20 mM meclofenamate Na had little influence in the properties of the solution, but this was not the case for higher drug concentrations. Diclofenac Na in a 1% (w/w) HPMC solution did not show significant changes in the flow behavior, but there was a change observed in the reduction of shear thinning at high shear rates. It was concluded that, at drug concentrations above 40 mM, the drug association improves the molecular hydration of the polymer [50]. The significant changes in the rheology of the sample at this drug concentration range show the formation of a weak supramolecular network through the strengthened interactions between polymer chains. As the concentration of meclofenamate Na increases, the drug begins to associate with the polymer conferring polyelectrolyte properties, and the solution viscosity increases as a result of coil expansion and increased connectivity between polymer chains. For diclofenac Na, the drug cannot associate enough to produce changes in the polymer solution properties.

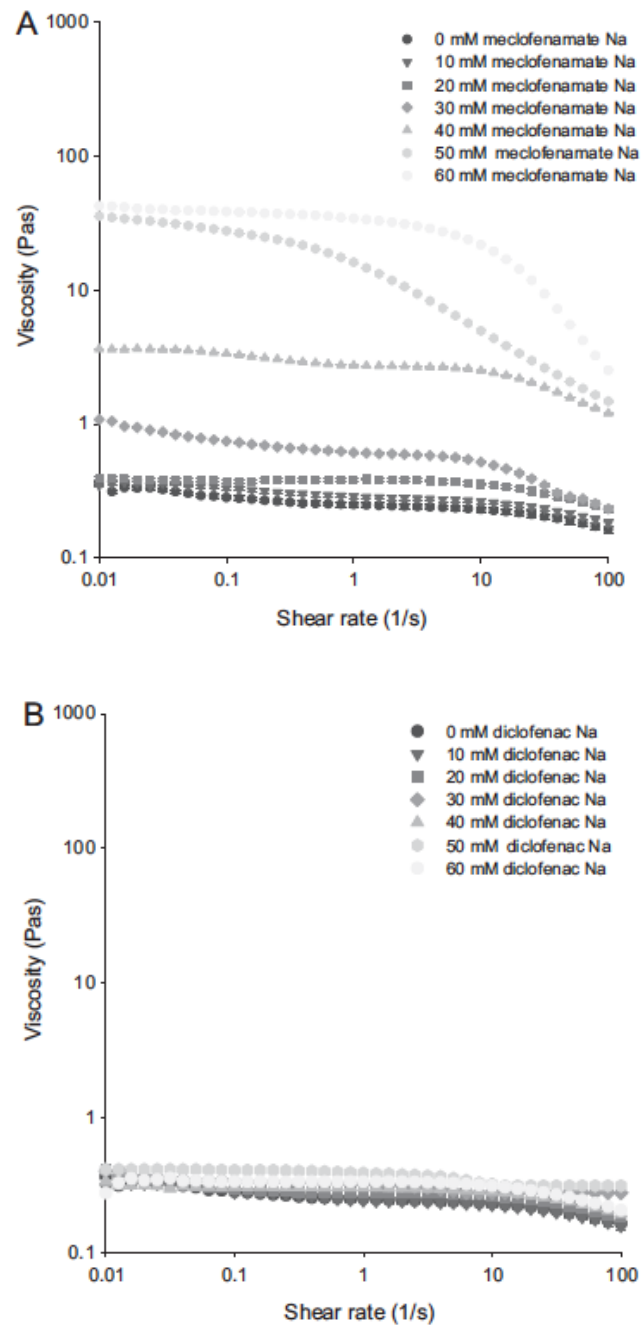


Figure 2.19: The continuous shear viscosity of 1% HPMC solutions with respect to drug concentration (A) meclufenamate Na and (B) diclofenac Na. Measurements at  $20 \pm 0.1^\circ\text{C}$ . Reproduced from [50].



Viriden and co-workers focused on the study of the effects of the chemical heterogeneity of HPMC on the release rate of a drug from matrix tablets [28]. Four different batches of HPMC with differing degree of substitution, molecular weight, and substituent heterogeneity, as summarized in Table 2.10, were used in their study.

Table 2.10: Polymer characteristics of the four HPMC batches. Reproduced from [28].

Sample	Mw (x 10 <sup>4</sup> g/mol)	P.I. (g/mol)	%HPO	%MeO
A	14.1 ± 0.3	2.8 ± 0.6	10.9	23.4
B	12.4 ± 0.1	2.8 ± 0.5	10.9	23.3
C	9.1 ± 0.0	1.9 ± 0.2	6.6	24.1
D	10.4 ± 0.2	2.2 ± 0.3	7.0	24.6

Viriden et al. performed flow curves, at 37 °C, in 5% and 10% (w/w) solutions. For 5% (w/w) solutions, an increase in viscosity was observed in the following order, A≈B<C<D, all throughout the shear rate interval (Figure 2.20) [28]. In addition, the viscosity increased with increased chemical heterogeneity. Thus, batch D demonstrated the highest viscosity. For the 10% (w/w) solutions, the same pattern was observed more prominently.

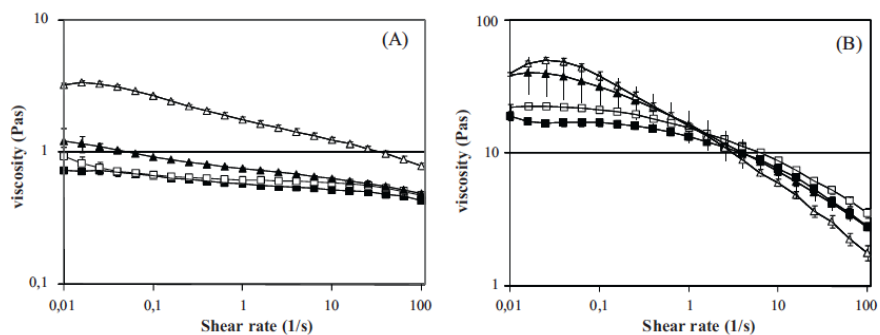


Figure 2.20: Flow curves obtained at 37°C. (A) 5% (w/w) HPMC solutions and (B) 10% (w/w) HPMC solutions. (■) Batch A, (□) Batch B, (filled  $\Delta$ ) Batch C and (open  $\Delta$ ) Batch D. Reproduced from [28].

Katzhendler and co-workers studied the effects of naproxen and naproxen sodium on HPMC matrices and the effects of the viscosity grade of HPMC has on the release of naproxen sodium (NS) from the matrix, and drug solubility on the release kinetics. The lowest viscosity grade used (i.e. K100LV) showed the highest release rate when compared to the higher viscosity grades (K4M and K100M). These higher viscosity grade HPMCs showed a similar release rate aside from their variation of molecular weight. The release of naproxen was controlled by surface erosion while the release of NS was mainly controlled by diffusion [51]. The release rate of naproxen, the lower soluble drug, was slower than the release rate of NS. For the diffusion of NS, there was little dependency on the HPMC viscosity grade, with the tendency for lower diffusion values with increasing HPMC viscosity grades; indicating that NS diffusion was exponentially dependent upon its own concentration.

### 2.3 BCS Class II Drugs

An important factor that needs to be taken into account during the development and design of new formulations is the solubility of the drug molecules [32,36]. Water-soluble drugs are released primarily by diffusion of dissolved drug molecules across the gel layer, while poorly water-soluble drugs are released predominantly by an erosion mechanism [36,51]. Particle size greatly influences the release rate of drugs that are poorly soluble due to the predominant mechanism of release [36]. The Biopharmaceutical Classification System (BCS) is the method used to classify the different types of drugs on the basis of their aqueous solubility and intestinal permeability [52,53]. The main objectives of the BCS classification system are (1) to improve the efficiency of the drug development and review process by recommending a strategy for identifying expendable clinical bioequivalence test; (2) to recommend a class of immediate-release solid oral dosage forms for which bioequivalence may be assessed based on in vitro dissolution test; and (3) to recommend methods for classification according to dosage form dissolution along with the solubility-permeability characteristics of the drug product [52]. The classification classes are listed in Table 2.11 below.

Table 2.11: The Biopharmaceutics Classification System.

<b>Class</b>	<b>Solubility</b>	<b>Permeability</b>
I	High	High
II	Low	High
III	High	Low
IV	Low	Low

The drugs used in this work are classified as BCS Class II drugs. These drugs are characterized by their poor solubility and high permeation in the human body [32,52–54]. The introduction of drugs into polymer films can alter its properties, like the viscosity and flowability of the polymer, which might lead to different functionalities of the film. The determination of critical properties of drug formulation become necessary to obtain the product with desired and reproducible attributes [43]. Drug release from the dosage form is controlled mainly by the properties of polymer and drug used in the preparations [34].

Table 2.12 includes some of the drugs with sufficient data to be characterized within the BCS classification system [55]. Of particular interest in this work is griseofulvin (highlighted in Table 2.12). Griseofulvin is a class II drug with low solubility and high permeability. Griseofulvin is a model BCS class II drug that has a inconsequential dissolution in water,  $\sim 10^{-5}$  M [11,56,57]. It is a commercial antifungal with low water solubility. The reported value for the zeta potential is  $-18.20 \pm 1.46$  mV [11,57].

Table 2.12: Classification of orally administered drugs on the WHO model list of Essential Medicines according to the BCS: *Drugs with reliable solubility and permeability data*. Reproduced from [55].

Drug	Solubility	Permeability	Dose (mg)	BCS class <sup>a</sup>
<b>Abacavir antiretroviral</b>	<b>High</b>	<b>Low</b>	<b>300 (sulfate)</b>	<b>III</b>
<b>Acetylsalicylic acid pain relief</b>	<b>High</b>	<b>Low</b>	<b>100–500</b>	<b>III<sup>*/**</sup></b>
<b>Aciclovir antiviral</b>	<b>High</b>	<b>Low</b>	<b>200</b>	<b>III</b>
<b>Allopurinol gout</b>	<b>High</b>	<b>Low</b>	<b>100</b>	<b>III</b>
Aluminium hydroxide gastro-intestinal agent	Low	Low	500	IV
<i>Amiloride diuretic</i>	<i>High</i>	<i>High</i>	<i>5 (hydrochloride)</i>	<i>I</i>
<b>Ascorbic acid vitamin</b>	<b>High</b>	<b>Low</b>	<b>50 (–1000)</b>	<b>III<sup>#</sup></b>
Atenolol $\beta$ -blocker	High	Low	50; 100	III
Captopril antihypertensive	High	Low	25	III
Carbamazepin antiepileptic	Low	High	100; 200	II
<b>Chloramphenicol antibiotic</b>	<b>High</b>	<b>Low</b>	<b>250</b>	<b>III</b>
<i>Chloroquine antimalarial agent</i>	<i>High</i>	<i>High</i>	<i>100 (Phosphate) 150 (Sulfate)</i>	<i>I</i>
Cimetidine H <sub>2</sub> -receptor antagonist	High	Low	200	III
Sodium Cloxacillin antibiotic	High	Low	500; 1000 (Na-salz)	III
<b>Codeine phosphate antitussive/analgetic</b>	<b>High</b>	<b>Low</b>	<b>30</b>	<b>III</b>
Colchicine antigout agent	High	Low	0.5	III
<i>Cyclophosphamide antineoplastic</i>	<i>High</i>	<i>High</i>	<i>25</i>	<i>I</i>
Dapsone antirheumatic/leprosy	Low	High	25; 50; 100	II
<i>Diazepam Benzodiazepine</i>	<i>High</i>	<i>High</i>	<i>2; 5</i>	<i>I</i>
<i>Digoxine cardiac glycoside</i>	<i>High</i>	<i>High</i>	<i>0.625; 0.25</i>	<i>I<sup>#</sup></i>
<i>Doxycycline antibiotic</i>	<i>High</i>	<i>High</i>	<i>100 (Hydrochlorid)</i>	<i>I</i>
Ergotamine Tartrate migraine	High	Low	1 (tartrate)	III*
<i>Fluconazole antifungal</i>	<i>High</i>	<i>High</i>	<i>50</i>	<i>I</i>
Furosemide diuretic	Low	Low	40	IV*
Griseofulvin antifungal	Low	High	125; 250	II
Hydralazine antihypertensive	High	Low	25; 50 (hydrochloride)	III*
Hydrochlorothiazide diuretic	High	Low	25	III

The other drug of interest in this work is naproxen, which is also classified as a class II drug [32]. Naproxen is a non-steroidal anti-inflammatory drug with poor solubility commonly used as an analgesic and for the treatment of symptoms, like those caused by rheumatoid arthritis and osteoarthritis and musculoskeletal pains [58–62]. The reported water solubility for naproxen is 15.9 mg/L at 25 °C [63].

## 2.4 Negative Deviation from the Einstein Viscosity Model

The addition of particles in a fluid affects its viscosity. The most basic model that predicts this phenomenon is the Einstein model:

$$\eta = \eta_s(1 + 2.5\phi)$$

which describes the shear viscosity of a suspension of non-interacting hard spheres [64,65]. This equation applies at low volume fractions ( $\phi \leq 0.03$ ) and when the suspension is sufficiently dilute that one sphere's flow behavior is not influenced nor affected by neighboring particles; in other words, it does not consider interaction between particles in Newtonian fluids. The Einstein model predicts an increase in the viscosity of a fluid with the addition of particles. This increase in viscosity is a function of the particle volume fraction and the viscosity of the suspending medium [65–67]. However, negative deviations from Einstein's prediction have been observed.

Mackay et al. [66] studied a system of polystyrene (PS) nanoparticles and linear polystyrene. They observed that the terminal viscosity of the system decreased with the addition of the nanoparticles, differing from the expected behavior predicted by the Einstein model. The observed decrease in viscosity was due to particle confinement. Therefore the addition of nanoparticles changed led to a decrease in viscosity.

Gao et al [68] studied the effect of nanotitania and nanocomposite particle loadings suspended in PS solutions. In the case of the suspensions with nanotitania particles above a concentration of 0.6 wt%, an increase in the steady viscosity and

shear thinning in the low shear rate area was observed. When comparing this with the nanocomposite particle suspension, a clear difference was observed. In this case, the initial loading of 0.6 wt% caused a decrease in the viscosity up to a concentration of 2.0 wt% where the behavior was very similar to that of pure PS. This behavior deviates from the one predicted by Stokes-Einstein. They attributed this decrease in viscosity to plasticization or dilution effects, excluded free volume, selective adsorption or constraint release [68].

Jain et al studied the effect of silica nanoparticle addition onto poly(propylene) (PP) at different compositions. They observed an initial decrease in the dynamic viscosity up to a concentration of 0.5 wt%; after that, it began to increase again [67]. The decrease in dynamic viscosity correlated to an extension of the Newtonian region. Furthermore, for all PP-silica nanocomposites mixtures, except 0.5 wt%, a shear thinning behavior was observed followed by shear thickening and shear thinning [67]. The viscosity reduction was attributed to selective physisorption of polymer chains of the highest molar mass on the nanoparticle surface [67]. Adsorption of high molar mass chains on the surface of nanoparticles eventually results in a reduction in entanglement density, therefore increasing the flowability or reducing the viscosity [67].

Oh and Green studied the effects the addition of gold nanoparticles on PS. Polymer nanocomposites (PNC) containing AuPS<sub>10</sub> showed a lower value of glass transition temperature ( $T_g$ ) than pure PS. In the case of the AuPS<sub>10</sub> nanocomposites, the  $T_g$  and dynamics were greatly influenced by two competing processes: well-

dispersed particles contribute to a  $T_g$  reduction and fast dynamics, while aggregation of the particles has the effect of reducing interfacial area and suppressing a further reduction in  $T_g$  and the further acceleration of dynamics [69].

Previous studies in our group also show a deviation from Einstein's behavior. Acevedo et al. studied the thermal gelation of hydroxypropylmethylcellulose (HPMC) solutions with SDS and hydrophobic drug particles. A decrease in viscosity was observed on the pure polymer with the addition of the griseofulvin particles, which led them to conclude that there is adsorption of the polymer onto the particle's surface. These deviations from the Einstein Model are typically observed with charged or hydrophobic particles. It is important to note that adsorption depends on the particle surface area; therefore, viscosity should be susceptible to particle size and distribution.



## Chapter 3

### Materials and Experimental Method

#### 3.1 Hydroxypropyl methylcellulose

In this work, the polymer studied was hydroxypropyl methylcellulose (HPMC) of two different viscosity grades, E4M (medium viscosity grade) and E15LV (low viscosity grade). Table 3.1 shows the properties provided by Sigma-Aldrich. The samples were used as received.

Table 3.1: Physical properties of HPMCs as provided by distributor

Viscosity Grade	Mn	Viscosity (mPa-s, 2% H <sub>2</sub> O at 25°C)	% methoxy substituents	% hydroxypropoxy substituents
E4M	86,000	3000-5600	28.0-30.0 %	7.0-12.0 %
E15LV	-	~ 15	-	~9%

<sup>1</sup>H-NMR-spectroscopy was performed for both E4M and E15LV viscosity grade HPMCs using the NMR Bruker 500 MHz spectrometer. The samples were prepared by dissolving the desired amount of HPMC in deuterated water (D<sub>2</sub>O) and then tested. The <sup>1</sup>H-NMR-spectra obtained for both HPMCs had the same signals at different intensities meaning that both viscosity grades have the same substituents groups present in different proportions. The signal observed at ~1.1 ppm is due to the methyl groups of the hydroxypropyl substituents that are attached to the carbon rather than the oxygen [46]. Haque et al. identified that the signals between ~2.0 and ~4.3

ppm, the resonances for the other protons in the hydroxypropyl substituents along with the protons of the methoxyl substituents and the protons of the cellulose chain.

### **3.2 BCS Class II Model Drugs: Griseofulvin and Naproxen**

The drugs used were griseofulvin and naproxen. Griseofulvin ((+)-Griseofulvin, 97%) was obtained from Alfa Aesar and was used as is. Naproxen from the inventory of the Pharmaceutical Engineering Laboratory at UPRM was used.

Zeta potential of HPMC solutions with griseofulvin and naproxen were performed at concentrations up to a 1:2 polymer to drug ratio at 0.025 wt% increments and constant temperature of 25 °C (Figure 3.1) using a Brookhaven Instrument 90 Plus Zeta Potential Analyzer. Additionally, zeta potential samples were prepared at fixed polymer concentration varying the drug concentration in 0.025 wt% increments until reaching a 1:2 polymer to drug ratio. For griseofulvin drug particles, an overall negative charge was observed for both HPMC viscosity grades. For naproxen, a negative charge was observed up to a drug concentration of 0.125 wt% where a small positive charge is beginning to be observed. Observed values were in the  $\pm 20$  mV range which indicates that the suspensions are not completely stable.

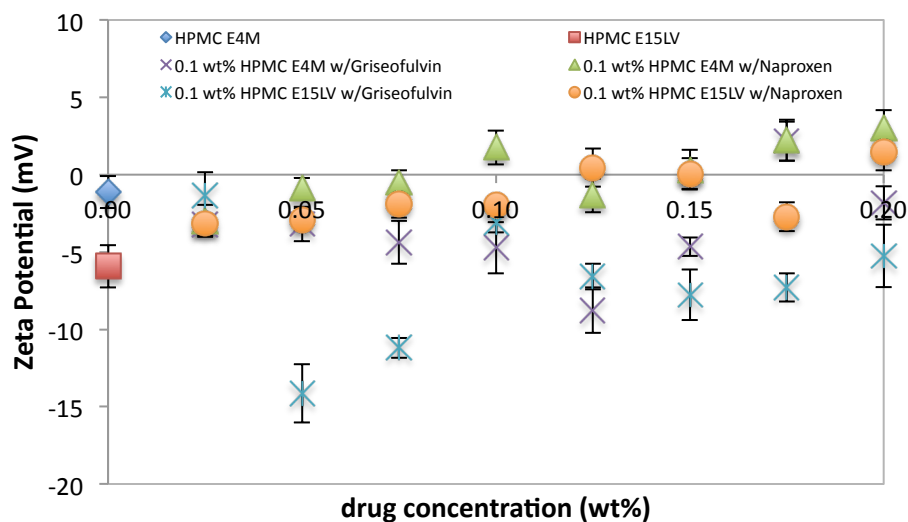


Figure 3.1: Zeta Potential for aqueous HPMC solutions with griseofulvin and naproxen

### 3.2.1 Drug Characterization

#### 3.2.1.1 Particle Size Determination

Dynamic light scattering was performed for griseofulvin drug particles using a Brookhaven Instrument 90 Plus Particle Size Analyzer in deionized water. The measured average hydrodynamic diameter was 207.6 nm.

The particle size of naproxen was determined using a Malvern Insitc Dry online particle size analyzer. To study the effect of particle size on the steady-state viscosity of HPMC solutions, naproxen was sieved using the RO-TAP RX-29 in order to obtain various ranges of particle size: > 125 micron, 75-125 micron, 45-75 micron

and < 45 micron. Figure 1 below shows the particle size distribution for sieved and unsieved naproxen.

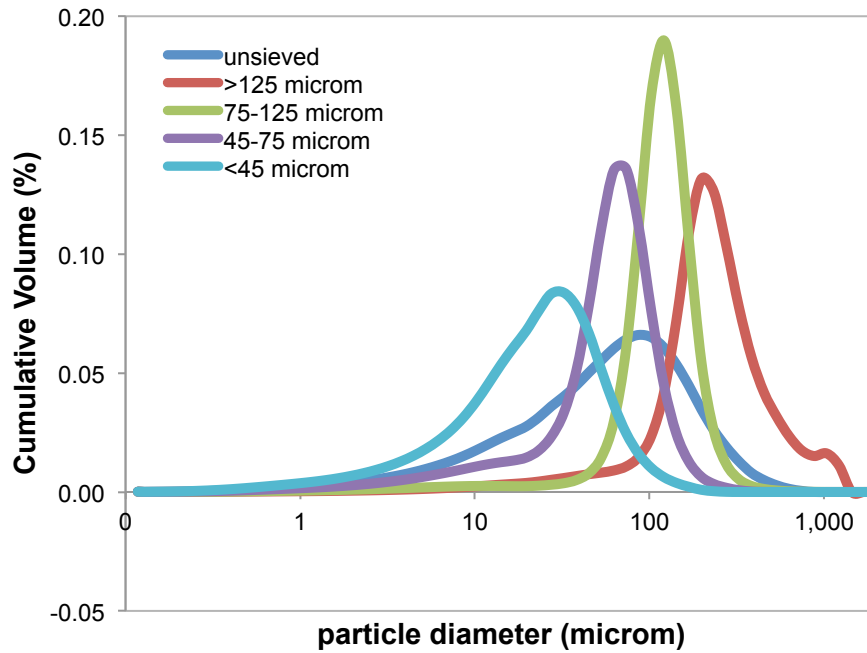


Figure 3.2: Particle size distribution for naproxen particles

Table 3.2: Particle size distribution for naproxen

Naproxen	Dv(10) micron	$\sigma$	Dv(50)* micron	$\sigma$	Dv(90) micron	$\sigma$
unsieved	8.200	0.767	56.820	4.005	178.780	19.668
<b>Sieved: particle size</b>						
>125 micron	85.330	12.293	204.130	22.174	491.490	143.978
75-125 micron	62.260	0.946	108.240	0.983	169.330	4.600
45-75 micron	13.110	1.152	56.680	0.808	101.430	3.958
<45 micron	4.610	0.432	21.550	0.618	53.190	3.485

\*Note: The Dv50 is the maximum particle diameter below which 50% of the volume exists.

### **3.2.1.2 Thermal Transitions**

A Texas Instrument DSC Q2000 was used to determine the thermal properties of the drugs. Samples weighing approximately 5 to 10 mg were used. The samples were tested under a nitrogen flow of 50 mL/min in a heating/cooling/heating cycle, with heating rates of 10 °C/min. The thermal degradation of the drugs was tested using a TGA/STDA 851 from Mettler Toledo. Samples weighing approximately 5 to 10 mg were used for these tests. Degradation temperatures were determined after heating the samples to 780 °C at 10 °C/min under airflow. From these test, the  $T_{\text{melt}}$  for griseofulvin and naproxen was determined to be 221°C and 150°C respectively.

### **3.3 HPMC Sample Preparation**

HPMC solutions were prepared by mixing the HPMC powder with deionized water to obtain the desired polymer concentration by weight. It was then heated and magnetically stirred at 40 °C for one hour and continued to be stirred at room temperature for at least 24 hours to dissolve the polymer completely. Drug particles were then added to the HPMC solution and sonicated in a Branson 250W sonicator (Branson Digital Sonifier 250W) for 20 to 25 minutes at a 10% amplitude.

Polymer concentration was fixed and the drug concentration was varied at 0.25 increments until reaching a ratio of 1:2 polymer to drug. The polymer concentrations used for E4M viscosity grade were 1 and 2 wt% and for E15LV was 2 wt%.

Equipment limitations inhibited the study of 1 wt% E15LV; therefore it could not be performed. Each sample was done in triplicate.

To study the effect of particle size on the steady-state viscosity of HPMC solutions, 2 wt% HPMC solutions of E4M and E15LV grade were prepared with the addition of naproxen particles in concentrations from 0 to 4 wt% at increments of 0.5 wt% for each sieve cut up to a 1:2 polymer to drug ratio. Thus, 9 samples per sieve cut in triplicate were evaluated.

### **3.3.1 Densitometry**

Solution density measurements were performed in an Anton Paar Density meter DMA 4100M at 25 °C. When the solution was too viscous for the equipment specifications, centrifugation of the samples was performed in a accuSpin 400 (Fischer Scientific) at 2000 rev/s for 10 minutes to remove any air within the sample, and weight and volume were recorded to calculate the density. Table 3.3 below shows the average solution densities for griseofulvin and naproxen in HPMC solutions (E4M and E15LV).

Table 3.3: Solution densities for Griseofulvin, unsieved Naproxen and sieved Naproxen in HPMC E4M and E15LV solutions

Drug	Density (g/cm <sup>3</sup> )		
	1 wt% HPMC E4M	2 wt% HPMC E4M	2 wt% HPMC E15LV
Griseofulvin	0.9977 ± 0.0020	0.9509 ± 0.0169	1.0032 ± 0.0051
Naproxen (unsieved)	1.0028 ± 0.0021	0.9470 ± 0.0233	1.0013 ± 0.0328
Naproxen <45 micron	1.0034 ± 0.0025	0.9472 ± 0.0149	1.0087 ± 0.0047
Naproxen 45- 75 micron	0.9980 ± 0.0119	0.9485 ± 0.0176	1.0088 ± 0.0049
Naproxen 75-125 micron	0.9996 ± 0.0105	0.9501 ± 0.0153	1.0089 ± 0.0049
Naproxen > 125 micron	1.0029 ± 0.0021	0.9415 ± 0.0213	1.0084 ± 0.0047

### 3.4 Rheological Measurements

In this work, steady state rheology was performed on an Anton Paar Physica MCR 302 rheometer using either a stainless steel double-gap Couette ( $V \approx 6$  mL), single Couette ( $V \approx 12$  mL), or parallel plates ( $d = 25$  mm) fixtures. The sample was allowed to relax for 20 minutes before performing the tests. Steady-state viscosity was measured using a shear rate ramp from 0.01 to 100  $s^{-1}$  at 25 °C. All measurements were done in triplicate.

## Chapter 4

### Results and Discussion

#### 4.1 Steady-state viscosity of HPMC solutions loaded with griseofulvin

The rheology of 2 wt% HPMC E15LV with griseofulvin particles was studied and an overall Newtonian behavior was observed (Figure 4.1) for particle concentration up to 4.0 wt%. No statistical significance in measured plateau viscosity was observed with the increasing addition of griseofulvin particles to the 2 wt% HPMC E15LV solution. This suggests that the addition of the griseofulvin particles does not affect the Newtonian viscosity for this particular polymer solution. Figure 4.2 shows the plateau viscosity values for HPMC E15LV solutions as a function of griseofulvin loading, where the error bars correspond to the standard deviation from multiple independent measurements.



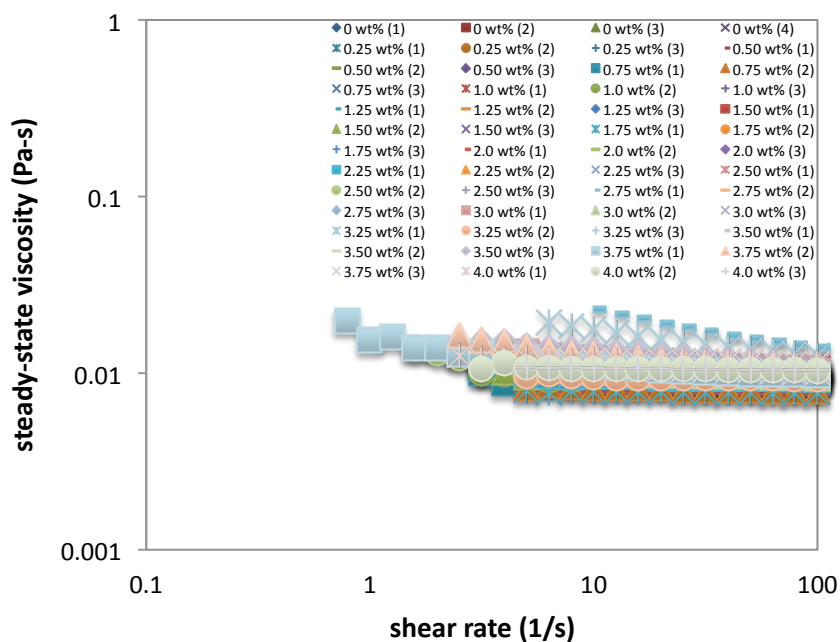


Figure 4.1: Steady-state viscosity of aqueous 2 wt% HPMC E15LV solution as a function of shear rate and griseofulvin concentration at 25°C

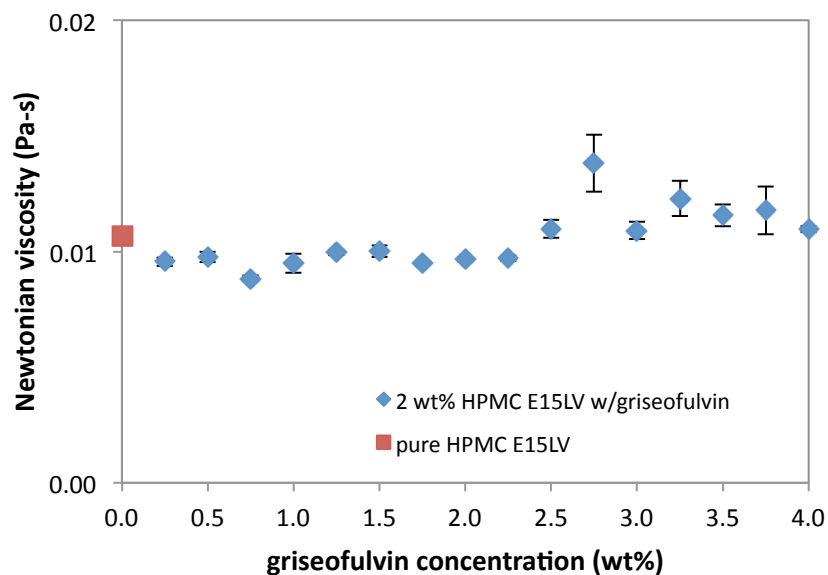


Figure 4.2: Newtonian viscosity for aqueous 2 wt% HPMC E15LV solution as a function of griseofulvin concentration at 25°C

In order to determine if the viscosity grade of the polymer plays a role in the rheology of the solution, HPMC E4M was studied under the same conditions. Figure 4.3, shows that the viscosity at low shear rate has shear thinning regime, which is followed by a plateau up to griseofulvin concentrations of 2.25 wt%. For solutions with higher concentrations, the plateau was not reached within the studied shear rate regime. The observed behavior is typically denoted as Bingham pseudo plastic, which can be described by the Bingham model. The Bingham model describes fluids that exhibit yield stresses and follows the following equation:

$$\eta(\dot{\gamma}) = \mu_0 + \frac{\tau_y}{\dot{\gamma}}$$

where  $\mu_0$  is the plateau viscosity of the fluid at high shear rate rage, and  $\tau_y$  is the yield stress. This type of fluids will not flow until a stress exceeding the yield stress is applied [70]. The data set in Figure 4.3 were fitted to the Bingham model treating  $\mu_0$  and  $\tau_y$  as adjustable parameters and minimizing the linear least squares error.

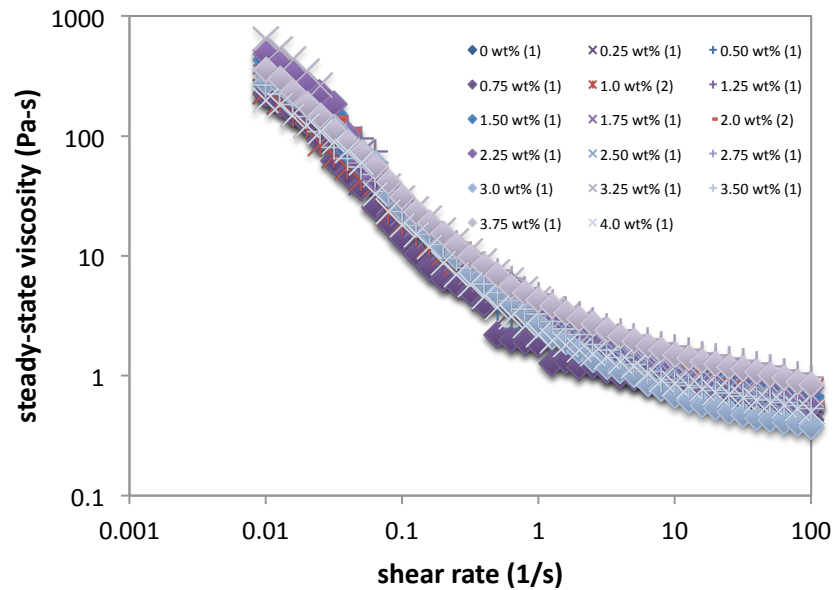


Figure 4.3: Steady-state viscosity of aqueous 2 wt% HPMC E4M solution as a function of shear rate and griseofulvin concentration at 25°C

Figure 4.4 summarizes the values of the fitted plateau viscosity of the Bingham model as a function of griseofulvin drug concentration on aqueous 2 wt% HPMC E4M solutions. The addition of griseofulvin particles decreases the viscosity of the HPMC solution by approximately a 0.6x factor. It is important to note that for drug concentrations above 2.25 wt%, no Newtonian behavior was observed. Figure 4.5 shows the effect of the addition of griseofulvin drug particles on the yield stress of the Bingham model for 2 wt% HPMC E4M solutions. The addition of griseofulvin particles lead to an initial decrease in the model yield stress by a 1/7x factor. As the concentration of griseofulvin increased, the yield stress remained under the obtained value for the HPMC solution. As has been discussed before the decrease in viscosity can be attributed to the adsorption of the polymer to the griseofulvin surface, which

reduces depletes the polymer from solution decreasing the effective viscosity of the continuous phase. Meanwhile, the changes in the yield stress are attributed to a decrease of polymer-polymer interaction that span the bulk of the fluid, which is also in agreement with adsorption of the polymer onto the drug surface. Since this effect is directly proportional to the depletion of polymer solution, maintaining the drug concentration fixed and decreasing the initial concentration of polymer will magnify the observed effect on viscosity and yield stress.

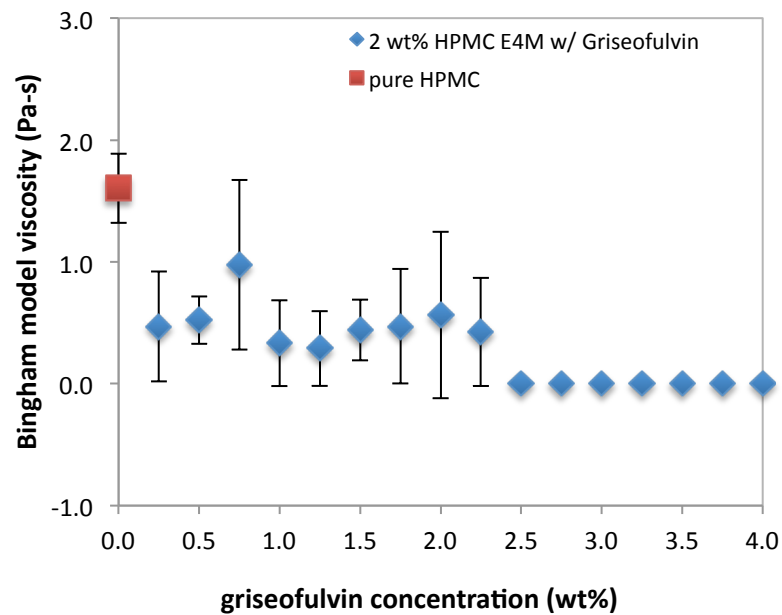


Figure 4.4: Plateau viscosity,  $\mu_0$ , from fitted Bingham model to steady-state viscosity of aqueous 2 wt% HPMC E4M solution as a function of shear rate and griseofulvin concentration at 25°C

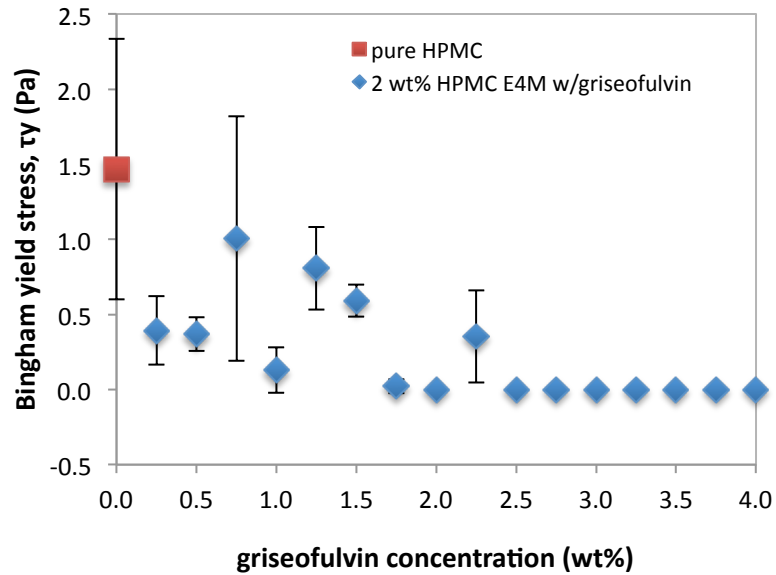


Figure 4.5: Yield stress,  $\tau_y$ , from fitted Bingham model to steady-state viscosity of aqueous 2 wt% HPMC E4M solution as a function of shear rate and griseofulvin concentration at 25°C

Figure 4.6 shows the steady state viscosity curves of 1wt% HPMC E4M solutions with griseofulvin particles. Similarly, a shear thinning behavior was observed followed by a Newtonian regime (for concentrations of up to 2 wt% of griseofulvin). For this polymer concentration, a larger decrease in the plateau viscosity, by a 1/7x factor, was observed with the initial addition of griseofulvin particles as shown in Figure 4.7. Further increases in particle concentration do not cause statistically significant differences on the plateau viscosity. Figure 4.8 shows the adjusted Bingham model yield stress for aqueous 1 wt% HPMC E4M solutions as a function of griseofulvin concentration. A decrease in the yield stress by a 1/7x factor was also observed with the addition of griseofulvin particles. This decrease in yield

stress indicates that the addition of griseofulvin particles decrease the yield stress needed for the initial solution to flow.

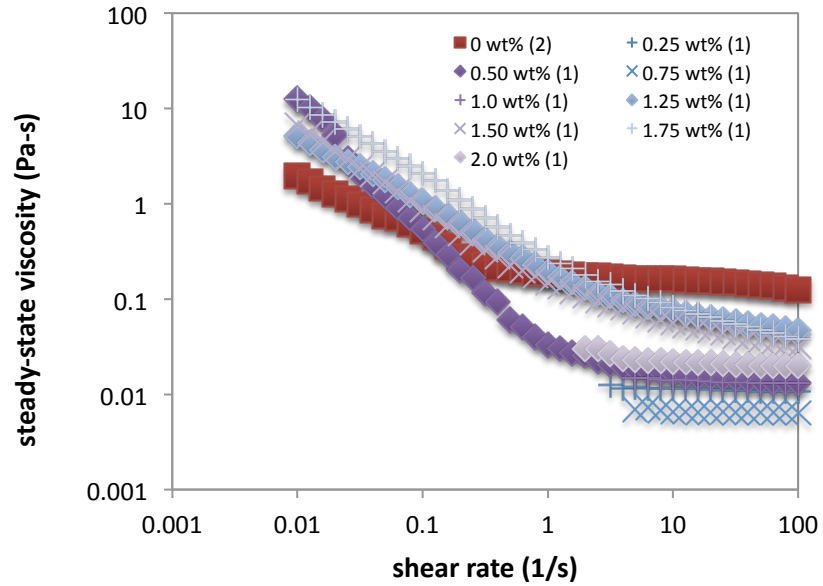


Figure 4.6: Steady-state viscosity of aqueous 1 wt% HPMC E4M solution as a function of shear rate and griseofulvin concentration at 25°C

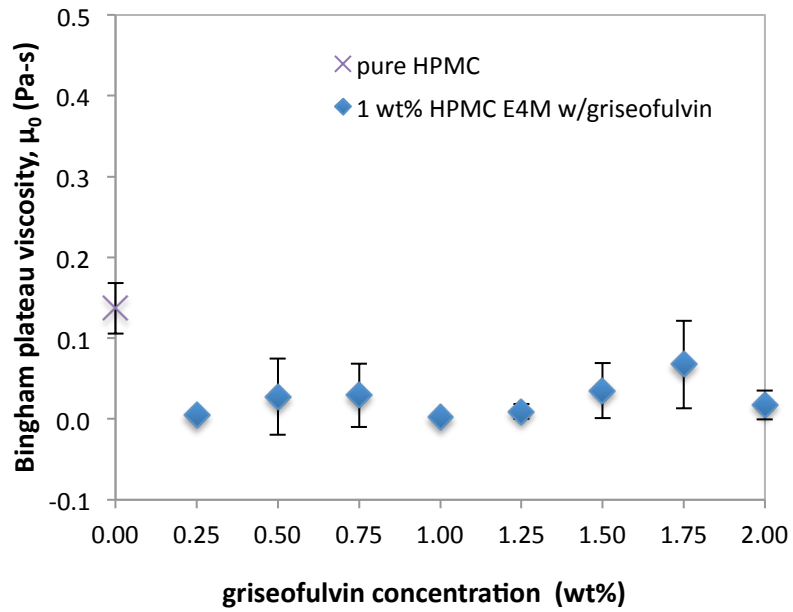


Figure 4.7: Plateau viscosity,  $\mu_0$ , from fitted Bingham model to steady-state viscosity of aqueous 2 wt% HPMC E4M solution as a function of shear rate and griseofulvin concentration at 25°C

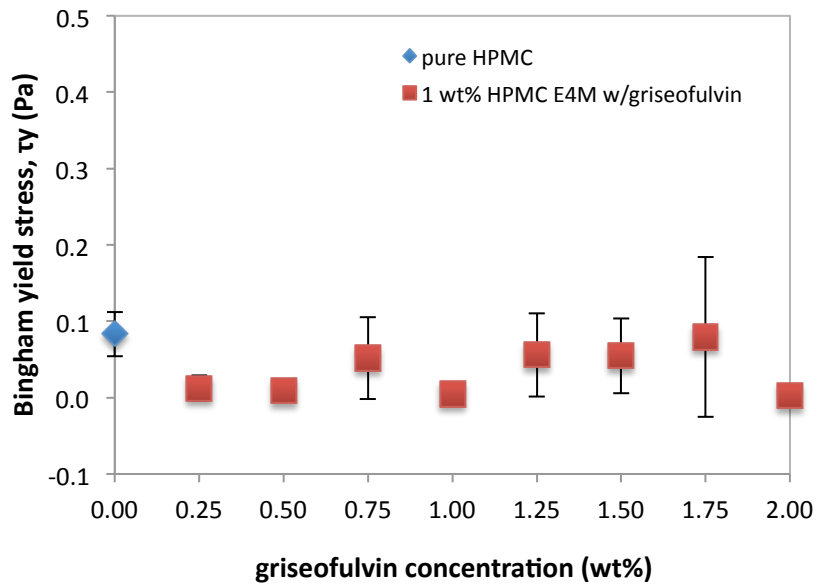


Figure 4.8: Adjusted yield stress,  $\tau_y$ , from fitted Bingham model to aqueous 1 wt% HPMC E4M solution as a function of griseofulvin concentration at 25°C

Both the 1 wt% and 2 wt% HPMC E4M solutions showed a decrease in viscosity upon addition of particles, which can be denoted as a deviation from the Einstein model. The behavior observed is in agreement to the previously reported by Acevedo et al [11] when studying the thermal gelation of HPMC solutions with SDS and hydrophobic drug particles which concluded that it was due to the adsorption of the polymer onto the particle's surface. Both parameters from the Bingham model, plateau viscosity and yield stress, showed larger decreases at lower polymer concentration which provides further proof that the phenomena is directly related to the overall surface area of the particles.

When comparing the molecular weight of the polymers, it was seen that for the lower viscosity grade polymer, only a Newtonian behavior was observed while for the medium viscosity grade a Bingham pseudoplastic behavior was observed. These results suggest that polymer entanglements are present for the higher molecular weight at the evaluated concentration. The polymer-polymer entanglements are disrupted with the addition of the griseofulvin particles and its effect diminished as evidenced by the decrease of the yield stress.

#### **4.2 Steady-state viscosity of HPMC solutions loaded with naproxen**

The rheology of HPMC solutions with naproxen particles, another BCS class II drug with similar properties- hydrophobic and insoluble- as griseofulvin, was evaluated to determine if the observed trends were generalizable or particle specific. In addition, the effect of particle size distribution was also evaluated using sieved cuts of naproxen.



The steady-state viscosity of 2 wt% HPMC E15LV was measured as a function of shear rate and unsieved naproxen concentration, which is summarized in Figure 4.9. A Newtonian behavior was observed throughout the evaluated shear rate range for all of the 2 wt% HPMC E15LV solutions, independently of the naproxen concentration (up to 4 wt%). Similar behavior was observed for all the sieved cuts naproxen dispersions (seen in Appendix). Figure 4.10 summarizes the measured effect in Newtonian viscosity with the addition of naproxen (unsieved and sieved cuts) to the polymer solution. An initial decrease of approximately 20% was observed, followed by an almost linear increase in viscosity as the concentration of naproxen particles increased. Even though the viscosity increases, its values did not surpass the viscosity of the pure HPMC E15LV. The addition of naproxen decreases the viscosity of the solution. No differences in behavior were observed when the particle size distribution was varied. The viscosity values were statistically the same between the unsieved and sieved cuts of naproxen.

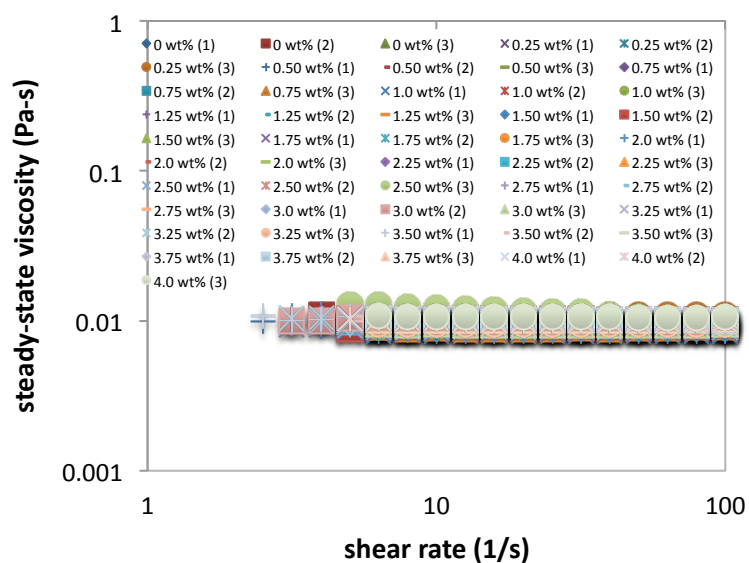


Figure 4.9: Steady-state viscosity of aqueous 2 wt% HPMC E15LV solution as a function of shear rate and naproxen concentration at 25°C

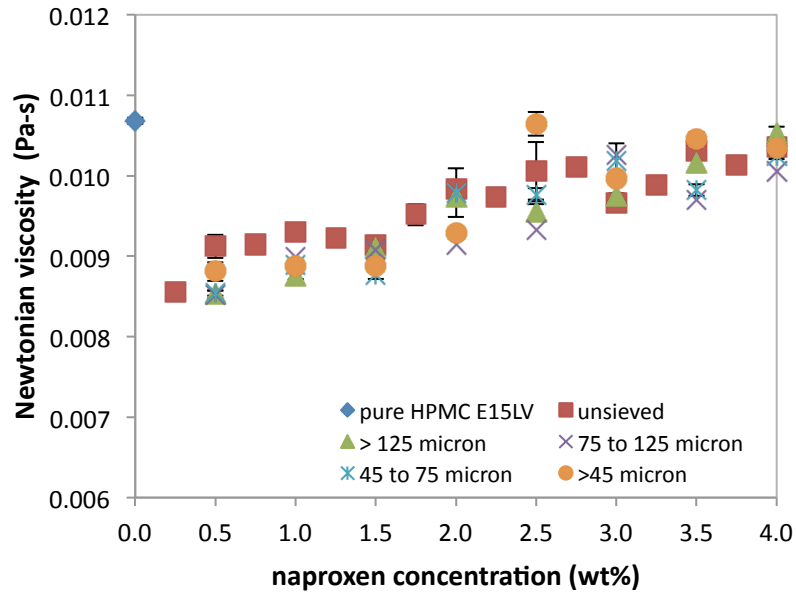


Figure 4.10: Newtonian viscosity for aqueous 2 wt% HPMC E15LV solution as a function of naproxen concentration (un-sieved and various particle size ranges: > 125 micron, 75 to 125 micron, 45 to 75 micron and <45 micron) at 25°C

Most of the 2 wt% HPMC E4M solutions showed a shear thinning regime followed by a Newtonian plateau that could be fitted to the Bingham model. Figure 4.11 and 4.12 show the adjusted plateau viscosity,  $\mu_0$ , and yield stress,  $\tau_y$ , from the Bingham model, respectively. A decrease in Newtonian viscosity was observed with the initial addition of naproxen particles by a factor of 1/6x. As the concentration of naproxen in solution increases, no significant variation was observed. Similar behavior was observed for unsieved and sieved cuts of naproxen. Therefore, the initial addition of naproxen affected the viscosity of HPMC but the increasing concentration of naproxen had no major effect. The addition of naproxen also reduced yield stress by a 1/7x factor; thus, less yield stress is needed for the solution to flow once naproxen has been dispersed in the solution. Similarly upon further increase of naproxen, the

yield stress did not show statistically significant differences. Neither does the particle size distribution have an effect on the yield stress of the solution.

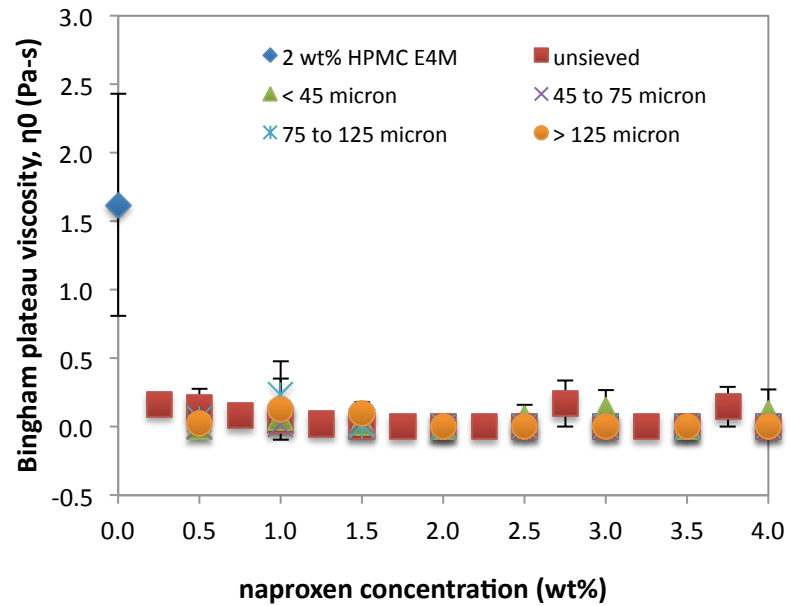


Figure 4.11: Plateau viscosity,  $\mu_0$ , from fitted Bingham model to steady-state viscosity of aqueous 2 wt% HPMC E4M solution as a function of shear rate and naproxen concentration (un-sieved and various particle size ranges: > 125 micron, 75 to 125 micron, 45 to 75 micron and <45 micron) at 25°C

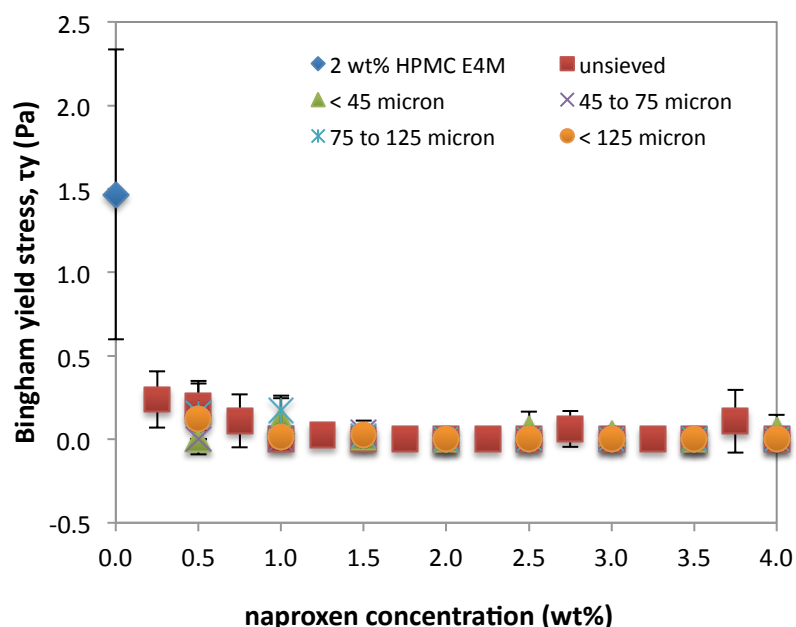


Figure 4.12: Adjusted yield stress,  $\tau_y$ , from fitted Bingham model to aqueous 2 wt% HPMC E4M solution as a function of naproxen (un-sieved and various particle size ranges: > 125 micron, 75 to 125 micron, 45 to 75 micron and <45 micron) at 25°C

Particle size distribution did not have an effect on the rheology of HPMC solutions. Comparing the distribution of sieved and unsieved naproxen shown in Figure 3.2 it can be gathered that the distributions are very broad and the ranges greatly overlap. Since in principle the macroscopic stress is due to the molecular contributions from all sizes, the overlap of the distribution suppresses the potential effect of particle size. When comparing the effects of griseofulvin and naproxen, it was seen that the general observation of decreased viscosity and yield stress was observed in both cases, but not to the same degree. This can be attributed to the effect of particle size of one drug and available surface. For instance, as previously mentioned, the average particle diameter for griseofulvin was measured to be 207.6 nm and for unsieved naproxen  $178.78 \pm 19.66$  micron; meaning that naproxen is bigger in size, therefore having less surface area than griseofulvin. The adsorption of

HPMC onto the particle surface leads to the reduction in viscosity observed, which is why we see a bigger reduction in viscosity for griseofulvin than for naproxen.

## Chapter 5

### **Conclusion**

The experiments presented in this work show that the interactions between water-insoluble BCS class II drugs and HPMC control its steady-state rheology. The two model drugs used, griseofulvin and naproxen, have the same effect, with slightly different magnitudes, on the rheological properties, a decrease in both viscosity and yield stress. Further evidence on the adsorption of HPMC on the particles surface was provided. The steady-state viscosity behavior was either Newtonian or pseudoplastic, which can be described by the Bingham model. Good agreement was obtained when fitting the experimental data to the Bingham model. Nevertheless, the data could not be adjusted to a single model that included the effects of polymer molecular weight, concentrations (polymer and drug), and drug particle size distribution. In fact, even when the effect of adsorption is directly proportional to the particle surface area, the use of commercial particles with broad distributions suppresses its effect.

In the broader context of the application for the production of drug loaded film casting from HPMC solutions, the results of this work allow us to draw some general guidelines on their formulation. The interactions of BSC Class II drugs with HPMC in solution will be similar due to their similar relevant physicochemical properties, hydrophobicity and low water solubility. Polymer adsorption onto the drug particles surface, which results in a reduction of the rheological properties due to depletion of polymer from the bulk, is most relevant only at low polymer concentrations. As polymer concentration is increased, the surface saturates and volumetric

hydrodynamic effects due to the presence of the particles predominate similar to a sterically stabilized suspension. Additionally, variations in size do not affect the rheological properties, especially when broad particle size distributions, typical of commercial particles, are used.

## REFERENCES

- [1] Y. S.R. Krishnaiah, Pharmaceutical Technologies for Enhancing Oral Bioavailability of Poorly Soluble Drugs, *J. Bioequivalence Bioavailab.* 02 (2010) 28–36. doi:10.4172/jbb.1000027.
- [2] P. Dorożyński, P. Kulinowski, A. Mendyk, R. Jachowicz, Gastroretentive drug delivery systems with l-dopa based on carrageenans and hydroxypropylmethylcellulose, *Int. J. Pharm.* 404 (2011) 169–175. doi:10.1016/j.ijpharm.2010.11.032.
- [3] R.P. Dixit, S.P. Puthli, Oral strip technology: Overview and future potential, *J. Controlled Release.* 139 (2009) 94–107. doi:10.1016/j.jconrel.2009.06.014.
- [4] F. Cilurzo, I.E. Cupone, P. Minghetti, F. Selmin, L. Montanari, Fast dissolving films made of maltodextrins, *Eur. J. Pharm. Biopharm.* 70 (2008) 895–900. doi:10.1016/j.ejpb.2008.06.032.
- [5] B. Vondrak, S. Barnhart, Dissolvable Films: DIssolvable Films for Flexible Product Format in Drug Delivery, *Pharm. Technol.* (2008).
- [6] P. Frey, Film Strips and Pharmaceuticals, *Pharm. Manuf. Pack. Sourcer.* (2006) 92–93.
- [7] V. Florián-Algarín, A. Acevedo, Rheology and Thermotropic Gelation of Aqueous Sodium Alginate Solutions, *J. Pharm. Innov.* 5 (2010) 37–44. doi:10.1007/s12247-010-9078-y.
- [8] D. Vaczek, New Routes in Drug Delivery, *Pharm. Med. Packag. News.* 15 (2007).
- [9] N.K. Sachan, S. Pushkar, A. Jha, A. Bhattacharya, Sodium alginate: the wonder polymer for controlled drug delivery, *J. Pharm. Res.* 2 (2009) 1191–1199.
- [10] V. Florián-Algarín, Rheology and Gelation of Physical Polymer Gels, University of Puerto Rico- Mayaguez Campus, 2011.
- [11] A. Acevedo, P. Takhistov, C.P. de la Rosa, V. Florián, Thermal gelation of aqueous hydroxypropylmethylcellulose solutions with SDS and hydrophobic drug particles, *Carbohydr. Polym.* 102 (2014) 74–79. doi:10.1016/j.carbpol.2013.11.017.
- [12] S. Bosselmann, R.O. Williams III, Chapter 1: Route-Specific Challenges in the Delivery of Poorly Water-Soluble Drugs, in: *Formul. Poorly Water Soluble Drugs*, Springer New York Dordrecht Heidelberg London, 2012: pp. 1–26.
- [13] V. Florian-Algarin, A. Acevedo, Effect of Silica Nanoparticles on Rheological Properties and Gelation Temperature of Biodegradable Polymer Gels, in: *Nano Science and Technology Institute ; CRC Press*, 2009: pp. 198–200.
- [14] C.A. Fyfe, A.I. Blazek, Investigation of Hydrogel Formation from Hydroxypropylmethylcellulose (HPMC) by NMR Spectroscopy and NMR



- Imaging Techniques, *Macromolecules*. 30 (1997) 6230–6237.  
doi:10.1021/ma970076o.
- [15] Nokhodchi, Ali, Raja, Shaista, Patel, Pryia, Asare-Addo, Kofi, The Role of Oral Controlled Release Matrix Tablets in Drug Delivery Systems, (2012).  
doi:10.5681/bi.2012.027.
- [16] S. Kamel, Pharmaceutical significance of cellulose: A review, *EXPRESS Polym. Lett.* 2 (2008) 758–778. doi:10.3144/expresspolymlett.2008.90.
- [17] S.M.C. Silva, F.V. Pinto, F.E. Antunes, M.G. Miguel, J.J.S. Sousa, A.A.C.C. Pais, Aggregation and gelation in hydroxypropylmethyl cellulose aqueous solutions, *J. Colloid Interface Sci.* 327 (2008) 333–340.  
doi:10.1016/j.jcis.2008.08.056.
- [18] S. Richardson, L. Gorton, Characterisation of the substituent distribution in starch and cellulose derivatives, *Anal. Chim. Acta.* 497 (2003) 27–65.  
doi:10.1016/j.aca.2003.08.005.
- [19] C. Clasen, W.-M. Kulicke, Determination of viscoelastic and rheo-optical material functions of water-soluble cellulose derivatives, *Progress Polym. Sci.* 26 (2001) 1839–1919.
- [20] G.S. Bajwa, C. Sammon, P. Timmins, C.D. Melia, Molecular and mechanical properties of hydroxypropyl methylcellulose solutions during the sol:gel transition, *Polymer*. 50 (2009) 4571–4576. doi:10.1016/j.polymer.2009.06.075.
- [21] N. Sarkar, L.C. Walker, Hydration—dehydration properties of methylcellulose and hydroxypropylmethylcellulose, *Carbohydr. Polym.* 27 (1995) 177–185.  
doi:10.1016/0144-8617(95)00061-B.
- [22] A. Viridén, B. Wittgren, A. Larsson, The consequence of the chemical composition of HPMC in matrix tablets on the release behaviour of model drug substances having different solubility, *Eur. J. Pharm. Biopharm.* 77 (2011) 99–110. doi:10.1016/j.ejpb.2010.11.004.
- [23] R. Bodvik, A. Dedinaite, L. Karlson, M. Bergström, P. Bäverbäck, J.S. Pedersen, et al., Aggregation and network formation of aqueous methylcellulose and hydroxypropylmethylcellulose solutions, *Colloids Surf. Physicochem. Eng. Asp.* 354 (2010) 162–171. doi:10.1016/j.colsurfa.2009.09.040.
- [24] Y. Yuguchi, H. Urakawa, S. Kitamura, S. Ohno, K. Kajiwara, Gelation mechanism of methylhydroxypropylcellulose in aqueous solution, *Food Hydrocoll.* 9 (1995) 173–179. doi:10.1016/S0268-005X(09)80213-0.
- [25] S. Hussain, C. Keary, D.Q.M. Craig, A thermorheological investigation into the gelation and phase separation of hydroxypropyl methylcellulose aqueous systems, *Polymer*. 43 (2002) 5623–5628.
- [26] A. Fatimi, J. François Tassin, S. Quillard, M.A.V. Axelos, P. Weiss, The rheological properties of silated hydroxypropylmethylcellulose tissue engineering matrices, *Biomaterials*. 29 (2008) 533–543.  
doi:10.1016/j.biomaterials.2007.10.032.

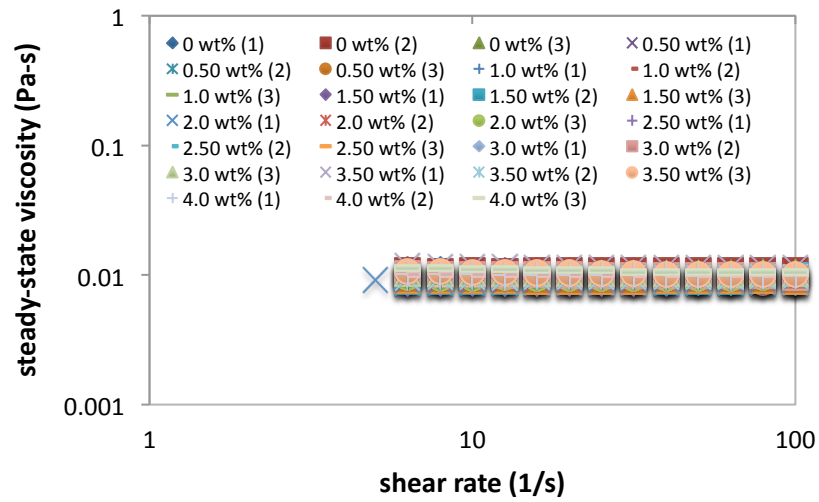
- [27] A. Ridell, H. Evertsson, S. Nilsson, L.-O. Sundelof, Amphiphilic association of ibuprofen and two nonionic cellulose derivatives in aqueous solution, *J. Pharm. Sci.* 88 (1999) 1175–1181. doi:10.1021/js990092u.
- [28] A. Viridén, A. Larsson, H. Schagerlöf, B. Wittgren, Model drug release from matrix tablets composed of HPMC with different substituent heterogeneity, *Int. J. Pharm.* 401 (2010) 60–67. doi:10.1016/j.ijpharm.2010.09.017.
- [29] M. Larsson, A. Viridén, M. Stading, A. Larsson, The influence of HPMC substitution pattern on solid-state properties, *Carbohydr. Polym.* 82 (2010) 1074–1081. doi:10.1016/j.carbpol.2010.06.030.
- [30] O. Chambin, D. Champion, C. Debray, M.H. Rochat-Gonthier, M. Le Meste, Y. Pourcelot, Effects of different cellulose derivatives on drug release mechanism studied at a preformulation stage, *J. Controlled Release.* 95 (2004) 101–108. doi:10.1016/j.jconrel.2003.11.009.
- [31] N. Sarkar, Thermal gelation properties of methyl and hydroxypropyl methylcellulose, *J. Appl. Polym. Sci.* 24 (1979) 1073–1087. doi:10.1002/app.1979.070240420.
- [32] L. Sievens-Figueroa, A. Bhakay, J.I. Jerez-Rozo, N. Pandya, R.J. Romañach, B. Michniak-Kohn, et al., Preparation and characterization of hydroxypropyl methyl cellulose films containing stable BCS Class II drug nanoparticles for pharmaceutical applications, *Int. J. Pharm.* 423 (2012) 496–508. doi:10.1016/j.ijpharm.2011.12.001.
- [33] J. Siepmann, N.A. Peppas, Modeling of drug release from delivery systems based on hydroxypropyl methylcellulose (HPMC), *Adv. Drug Deliv. Rev.* 64 (2012) 163–174. doi:10.1016/j.addr.2012.09.028.
- [34] S. Devjak Novak, E. Šporar, S. Baumgartner, F. Vrečer, Characterization of physicochemical properties of hydroxypropyl methylcellulose (HPMC) type 2208 and their influence on prolonged drug release from matrix tablets, *J. Pharm. Biomed. Anal.* 66 (2012) 136–143. doi:10.1016/j.jpba.2012.03.032.
- [35] S.R. Pygall, S. Kujawinski, P. Timmins, C.D. Melia, Mechanisms of drug release in citrate buffered HPMC matrices, *Int. J. Pharm.* 370 (2009) 110–120. doi:10.1016/j.ijpharm.2008.11.022.
- [36] C.L. Li, L.G. Martini, J.L. Ford, M. Roberts, The use of hypromellose in oral drug delivery, *J. Pharm. Pharmacol.* 57 (2005) 533–546. doi:10.1211/0022357055957.
- [37] S.R. Pygall, S. Kujawinski, P. Timmins, C.D. Melia, The suitability of tris(hydroxymethyl) aminomethane (THAM) as a buffering system for hydroxypropyl methylcellulose (HPMC) hydrophilic matrices containing a weak acid drug, *Int. J. Pharm.* 387 (2010) 93–102. doi:10.1016/j.ijpharm.2009.12.012.
- [38] S.C. Joshi, Sol-Gel Behavior of Hydroxypropyl Methylcellulose (HPMC) in Ionic Media Including Drug Release, *Materials.* 4 (2011) 1861–1905. doi:10.3390/ma4101861.

- [39] A. Viridén, B. Wittgren, A. Larsson, Investigation of critical polymer properties for polymer release and swelling of HPMC matrix tablets, *Eur. J. Pharm. Sci.* 36 (2009) 297–309. doi:10.1016/j.ejps.2008.10.021.
- [40] O.E. Pérez, V. Wargon, A. M.R. Pilosof, Gelation and structural characteristics of incompatible whey proteins/hydroxypropylmethylcellulose mixtures, *Food Hydrocoll.* 20 (2006) 966–974. doi:10.1016/j.foodhyd.2005.11.005.
- [41] A. Viridén, B. Wittgren, T. Andersson, S. Abrahmsén-Alami, A. Larsson, Influence of Substitution Pattern on Solution Behavior of Hydroxypropyl Methylcellulose, *Biomacromolecules.* 10 (2009) 522–529. doi:10.1021/bm801140q.
- [42] A. Viridén, B. Wittgren, T. Andersson, A. Larsson, The effect of chemical heterogeneity of HPMC on polymer release from matrix tablets, *Eur. J. Pharm. Sci.* 36 (2009) 392–400. doi:10.1016/j.ejps.2008.11.003.
- [43] S. Piriyaarasath, P. Sriamornsak, Effect of source variation on drug release from HPMC tablets: Linear regression modeling for prediction of drug release, *Int. J. Pharm.* 411 (2011) 36–42. doi:10.1016/j.ijpharm.2011.03.019.
- [44] H. Akinosho, S. Hawkins, L. Wicker, Hydroxypropyl methylcellulose substituent analysis and rheological properties, *Carbohydr. Polym.* 98 (2013) 276–281. doi:10.1016/j.carbpol.2013.05.081.
- [45] N.A. Camino, O.E. Pérez, A.M.R. Pilosof, Molecular and functional modification of hydroxypropylmethylcellulose by high-intensity ultrasound, *Food Hydrocoll.* 23 (2009) 1089–1095. doi:10.1016/j.foodhyd.2008.08.015.
- [46] A. Haque, R.K. Richardson, E.R. Morris, M.J. Gidley, D.C. Caswell, Thermogelation of methylcellulose. Part II: effect of hydroxypropyl substituents, *Carbohydr. Polym.* 22 (1993) 175–186. doi:10.1016/0144-8617(93)90138-T.
- [47] A. Haque, E.R. Morris, Thermogelation of methylcellulose. Part I: molecular structures and processes, *Carbohydr. Polym.* 22 (1993) 161–173. doi:10.1016/0144-8617(93)90137-S.
- [48] J. Ford, Thermal analysis of hydroxypropylmethylcellulose and methylcellulose: powders, gels and matrix tablets, *Int. J. Pharm.* 179 (1999) 209–228. doi:10.1016/S0378-5173(98)00339-1.
- [49] M. Kawaguchi, Y. Ryo, Rheological properties of silica suspensions in aqueous cellulose derivative solutions, *Chem. Eng. Sci.* 48 (1993) 393–400. doi:10.1016/0009-2509(93)80024-K.
- [50] S.R. Pygall, P.C. Griffiths, B. Wolf, P. Timmins, C.D. Melia, Solution interactions of diclofenac sodium and meclofenamic acid sodium with hydroxypropyl methylcellulose (HPMC), *Int. J. Pharm.* 405 (2011) 55–62. doi:10.1016/j.ijpharm.2010.11.043.
- [51] I. Katzhendler, K. Mäder, M. Friedman, Structure and hydration properties of hydroxypropyl methylcellulose matrices containing naproxen and naproxen sodium, *Int. J. Pharm.* 200 (2000) 161–179. doi:10.1016/S0378-5173(00)00360-4.
- [52] B.B.K. Reddy, A. Karunakai, Biopharmaceutics Classification System: A Regulatory Approach, *Dissolution Technol.* (2011) 31–37.

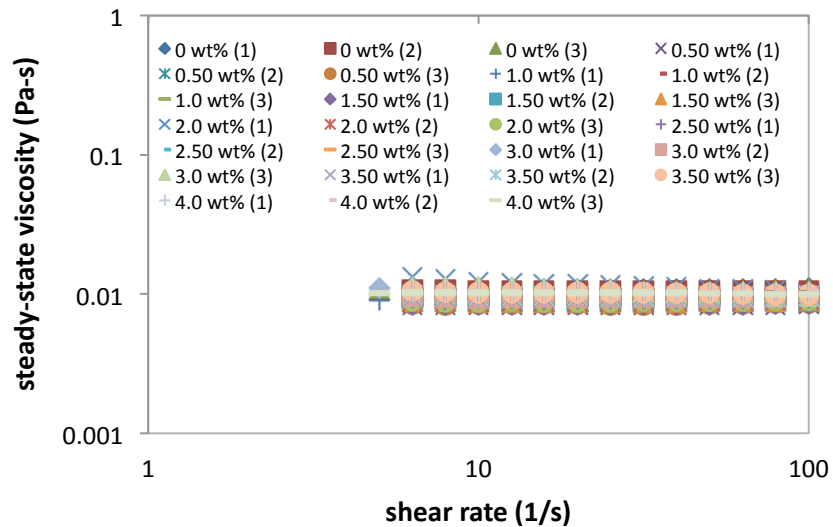
- [53] Guidance for Industry: Waiver of In Vivo Bioavailability and Bioequivalence Studies for Immediate-Release Solid Oral Dosage Forms Based on a Biopharmaceutics Classification System, (2000).
- [54] D. Bolten, R. Lietzow, M. Türk, Solubility of Ibuprofen, Phytosterol, Salicylic Acid, and Naproxen in Aqueous Solutions, *Chem. Eng. Technol.* 36 (2013) 426–434. doi:10.1002/ceat.201200510.
- [55] M. Lindenberg, S. Kopp, J.B. Dressman, Classification of orally administered drugs on the World Health Organization Model list of Essential Medicines according to the biopharmaceutics classification system, *Eur. J. Pharm. Biopharm.* 58 (2004) 265–278.
- [56] E. Rytting, K.A. Lentz, X.-Q. Chen, F. Qian, S. Venkatesh, Aqueous and cosolvent solubility data for drug-like organic compounds, *AAPS J.* 7 (2005) E78–E105. doi:10.1208/aapsj070110.
- [57] K. Itoh, A. Pongpeerapat, Y. Tozuka, T. Oguchi, K. Yamamoto, Nanoparticle Formation of Poorly Water-Soluble Drugs from Ternary Ground Mixtures with PVP and SDS, *Chem. Pharm. Bull. (Tokyo)*. 51 (2003) 171–174. doi:10.1248/cpb.51.171.
- [58] Ç. Sarıcı-Özdemir, Y. Önal, Study to investigate the importance of mass transfer of naproxen sodium onto activated carbon, *Chem. Eng. Process. Process Intensif.* 49 (2010) 1058–1065. doi:10.1016/j.cep.2010.08.011.
- [59] C.P. Mora, F. Martínez, Solubility of naproxen in several organic solvents at different temperatures, *Fluid Phase Equilibria*. 255 (2007) 70–77. doi:10.1016/j.fluid.2007.03.029.
- [60] Z. Guo, X.-M. Liu, L. Ma, J. Li, H. Zhang, Y.-P. Gao, et al., Effects of particle morphology, pore size and surface coating of mesoporous silica on Naproxen dissolution rate enhancement, *Colloids Surf. B Biointerfaces*. 101 (2013) 228–235. doi:10.1016/j.colsurfb.2012.06.026.
- [61] P. Di Martino, C. Barthélémy, G.F. Palmieri, S. Martelli, Physical characterization of naproxen sodium hydrate and anhydrate forms, *Eur. J. Pharm. Sci. Off. J. Eur. Fed. Pharm. Sci.* 14 (2001) 293–300.
- [62] Y. Javadzadeh, F. Ahadi, S. Davaran, G. Mohammadi, A. Sabzevari, K. Adibkia, Preparation and physicochemical characterization of naproxen–PLGA nanoparticles, *Colloids Surf. B Biointerfaces*. 81 (2010) 498–502. doi:10.1016/j.colsurfb.2010.07.047.
- [63] Z. Yu, S. Peldszus, P.M. Huck, Adsorption characteristics of selected pharmaceuticals and an endocrine disrupting compound—Naproxen, carbamazepine and nonylphenol—on activated carbon, *Water Res.* 42 (2008) 2873–2882. doi:10.1016/j.watres.2008.02.020.
- [64] R.G. Larson, *The structure and rheology of complex fluids*, Oxford University Press, New York, 1999.
- [65] A. Tuteja, M.E. Mackay, C.J. Hawker, B. Van Horn, Effect of Ideal, Organic Nanoparticles on the Flow Properties of Linear Polymers: Non-Einstein-like Behavior, *Macromolecules*. 38 (2005) 8000–8011. doi:10.1021/ma050974h.

- [66] M.E. Mackay, T.T. Dao, A. Tuteja, D.L. Ho, B. Van Horn, H.-C. Kim, et al., Nanoscale effects leading to non-Einstein-like decrease in viscosity, *Nat. Mater.* 2 (2003) 762–766. doi:10.1038/nmat999.
- [67] S. Jain, J.G.P. Goossens, G.W.M. Peters, M. van Duin, P.J. Lemstra, Strong decrease in viscosity of nanoparticle-filled polymer melts through selective adsorption, *Soft Matter.* 4 (2008) 1848. doi:10.1039/b802905a.
- [68] Y. Gao, Y. Song, Q. Zheng, Miniemulsion polymerized titania/polystyrene core-shell nanocomposite particles based on nanotitania powder: Morphology, composition and suspension rheology, *Colloids Surf. Physicochem. Eng. Asp.* 411 (2012) 40–49. doi:10.1016/j.colsurfa.2012.06.043.
- [69] H. Oh, P.F. Green, Polymer chain dynamics and glass transition in athermal polymer/nanoparticle mixtures, *Nat. Mater.* 8 (2009) 139–143. doi:10.1038/nmat2354.
- [70] F.A. Morrison, *Understanding Rheology*, Oxford University Press, New York, 2001.

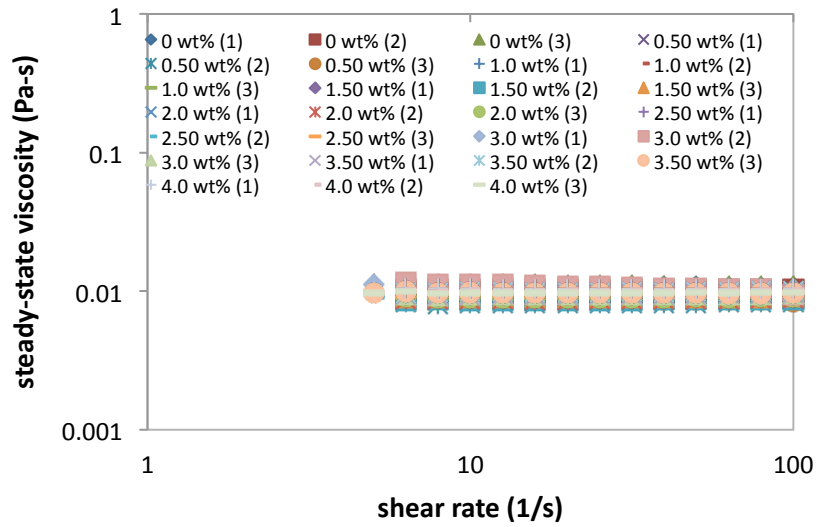
## APPENDIX



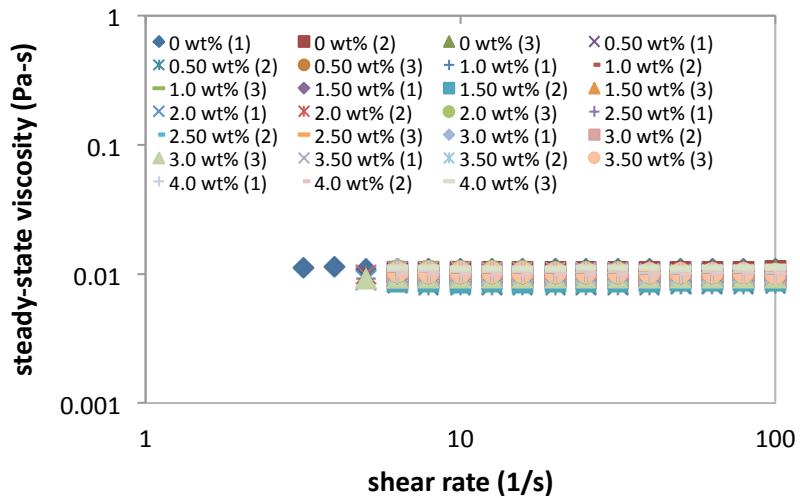
Appendix 1: Steady-state viscosity of aqueous 2 wt% HPMC E15LV solution as a function of shear rate and naproxen particle concentration (<45 micron) at 25°C



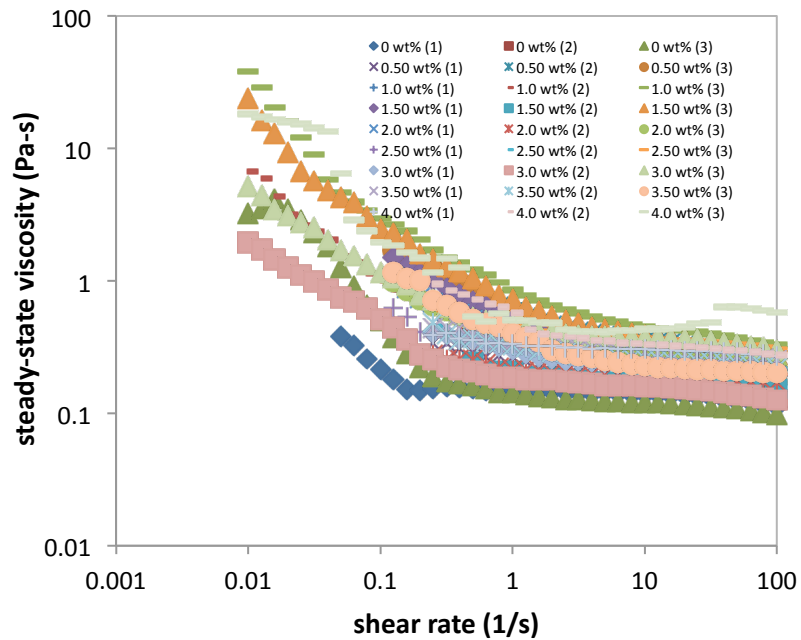
Appendix 2: Steady-state viscosity of aqueous 2 wt% HPMC E15LV solution as a function of shear rate and naproxen particle concentration (45 to 75 micron) at 25°C



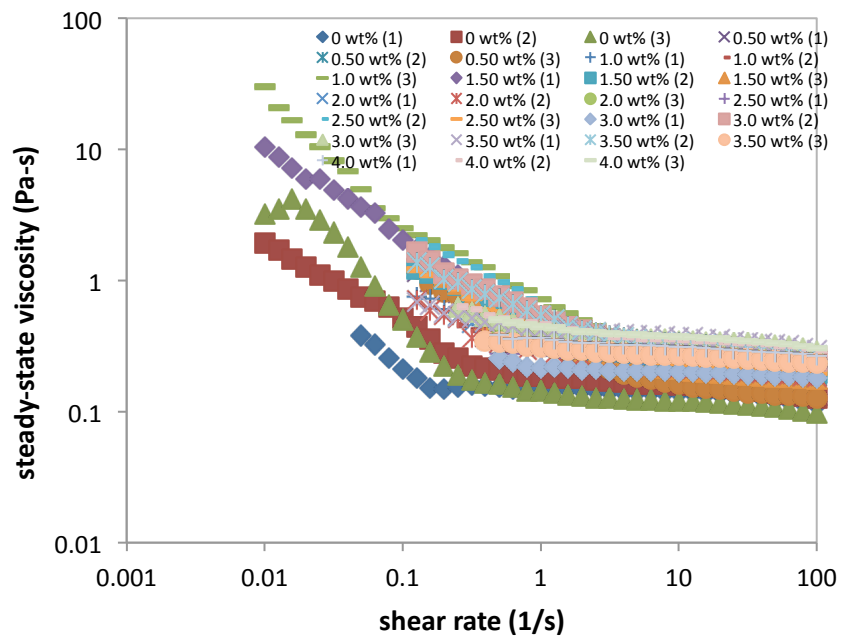
Appendix 3: Steady-state viscosity of aqueous 2 wt% HPMC E15LV solution as a function of shear rate and naproxen particle concentration (75 to 125 micron) at 25°C



Appendix 4: Steady-state viscosity of aqueous 2 wt% HPMC E15LV solution as a function of shear rate and naproxen concentration (>125 micron) at 25°C

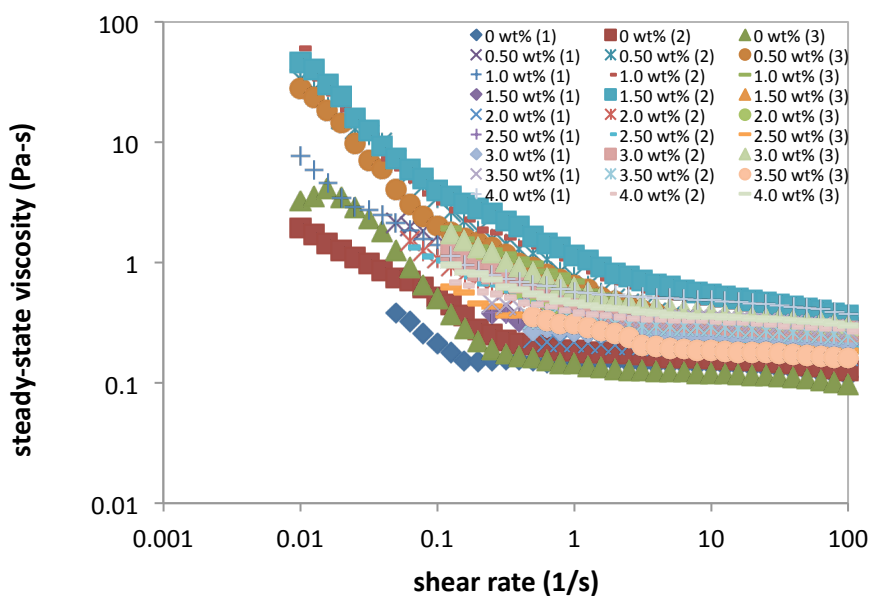


Appendix 5: Steady-state viscosity of aqueous 2 wt% HPMC E4M solution as a function of shear rate and naproxen concentration (< 45 micron) at 25°C

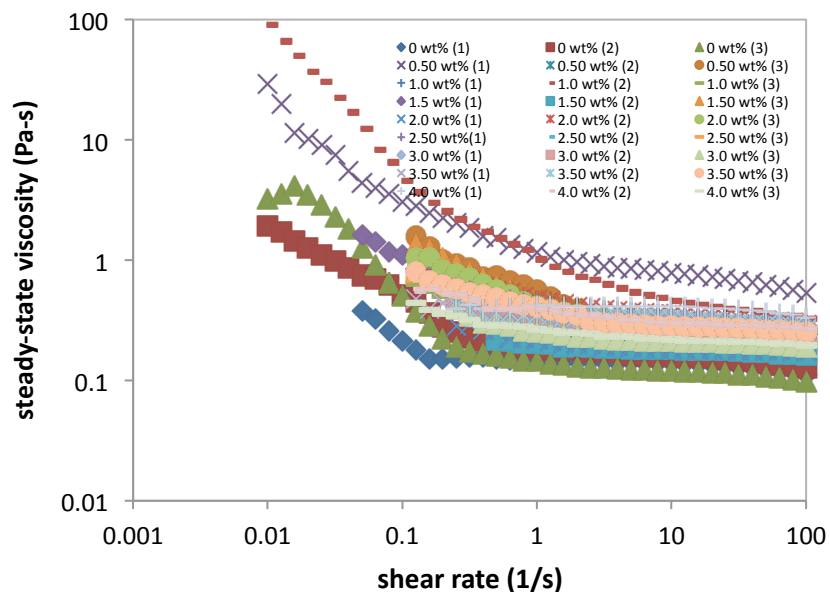


Appendix 6: Steady-state viscosity of aqueous 2 wt% HPMC E4M solution as a function of shear rate and naproxen (45 to 75 micron) at 25°C





Appendix 7: Steady-state viscosity of aqueous 2 wt% HPMC E4M solution as a function of shear rate and naproxen (75 to 125 micron) at 25°C



Appendix 8: Steady-state viscosity of aqueous 2 wt% HPMC E4M solution as a function of shear rate and naproxen concentration (> 125 micron) at 25°C